Dalton Transactions

PAPER

View Article Online
View Journal | View Issue

Open Access Article. Published on 11 February 2016. Downloaded on 10/20/2025 7:02:02 PM.
This article is licensed under a Creative Commons Attribution 3.0 Unported Licence.

Cite this: *Dalton Trans.*, 2016, **45**, 5122

# Coinage metal complexes with bridging hybrid phosphine–NHC ligands: synthesis of di- and tetra-nuclear complexes†‡

Thomas Simler,[a] Pierre Braunstein*[a] and Andreas A. Danopoulos*[a,b]

A series of P–NHC-type hybrid ligands containing both $PR_2$ and N-heterocyclic carbene (NHC) donors on *meta*-bis-substituted phenylene backbones, $\mathbf{L^{Cy}}$, $\mathbf{L^{tBu}}$ and $\mathbf{L^{Ph}}$ (R = Cy, *t*Bu, Ph, respectively), was accessed through a modular synthesis from a common precursor, and their coordination chemistry with coinage metals was explored and compared. Metallation of $\mathbf{L^{Ph}}\cdot n$(HBr) ($n$ = 1, 2) with $Ag_2O$ gave the pseudo-cubane $[Ag_4Br_4(\mathbf{L^{Ph}})_2]$, isostructural to $[Ag_4Br_4(\mathbf{L^{R}})_2]$ (R = Cy, *t*Bu) (T. Simler, P. Braunstein and A. A. Danopoulos, *Angew. Chem., Int. Ed.*, 2015, **54**, 13691), whereas metallation of $\mathbf{L^{R}}\cdot HBF_4$ (R = Ph, *t*Bu) led to the dinuclear complexes $[Ag_2(\mathbf{L^{R}})_2](BF_4)_2$ which, in the solid state, feature heteroleptic Ag centres and a 'head-to-tail' (HT) arrangement of the bridging ligands. In solution, interconversion with the homoleptic 'head-to-head' (HH) isomers is facilitated by ligand fluxionality. 'Head-to-tail' $[Cu_2Br_2(\mathbf{L^{R}})_2]$ (R = Cy, *t*Bu) dinuclear complexes were obtained from $\mathbf{L^{R}}\cdot$HBr and $[Cu_5(Mes)_5]$, Mes = 2,4,6-trimethylphenyl, which also feature bridging ligands and heteroleptic Cu centres. Although the various ligands $\mathbf{L^{R}}$ led to structurally analogous complexes for R = Cy, *t*Bu and Ph, the rates of dynamic processes occurring in solution are dependent on R, with faster rates for R = Ph. Transmetallation of both NHC and P donor groups from $[Ag_4Br_4(\mathbf{L^{tBu}})_2]$ to $Au^{I}$ by reaction with [AuCl(THT)] (THT = tetrahydrothiophene) led to $\mathbf{L^{tBu}}$ transfer and to the dinuclear complex $[Au_2Cl_2\mathbf{L^{tBu}}]$ with one $\mathbf{L^{tBu}}$ ligand bridging the two Au centres. Except for the silver pseudo-cubanes, all other complexes do not exhibit metallophilic interactions.

Received 20th January 2016,
Accepted 11th February 2016

DOI: 10.1039/c6dt00275g

www.rsc.org/dalton

## Introduction

Phosphine and NHC donors are often compared because they readily coordinate to metal centres and display bonding analogies and tuneable stereo-electronic properties.[1] However, despite the fact that both are considered as strong σ-donors, emerging evidence reveals subtly different σ-donating and π-accepting properties, diversifying across the periodic table.[2] This can lead to transition metal complexes with beneficial catalytic properties, *e.g.* finely controlled lability and metal electronic tuning, stability of the catalytically active species *etc.* The complementary roles of both types of donors participating in the same metal coordination sphere may enhance synergism,[3] although counter examples have been described.[4] The beneficial synergism may be enhanced if the hetero donors are part of a hybrid ligand. This background justifies synthetic efforts towards the design of new phosphine-functionalised NHC (P–NHC) complexes,[5] with reported high activities in C–C coupling reactions ($Pd^{II}$, $Ir^{I}$),[6] amination of aryl chlorides ($Pd^{II}$)[7] and transfer hydrogenation of ketones ($Ru^{II}$).[8]

Among the P–NHC-type ligands, bidentate hybrid ligands with direct P–N bond,[9] flexible alkyl,[6a–c,f,8,10] or more rigid and tuneable aryl spacer between the donors, **1a** and **1b**, respectively, have attracted most attention (Fig. 1);[6d,7,11] in particular, we and others have been interested in the *meta*-bis-substituted phenylene framework **1c–1d** as potential precursor to non-symmetrical $PCC^{NHC}$ 'pincer' complexes.[12] Relevant $PC^{NHC}P$ pincer and $P_2(C^{NHC})_2$ macrocyclic ligands **2**[6f,9c,13] and **3**,[5a] respectively, have been described.

The coordination chemistry of P–NHC-type ligands has mainly been focussed on late transition metals; the few structurally characterized examples[14] incorporating $Ag^{I}$,[9a,c,10g,11a,12a,c,e,15] or $Cu^{I}$ are depicted in Fig. 2.[9c,10f,12e,13b,15c] This relative scarcity is surprising, considering the interest for air stable group 11 NHC

[a]*Laboratoire de Chimie de Coordination, Institut de Chimie (UMR 7177 CNRS), Université de Strasbourg, 4 rue Blaise Pascal, 67081 Strasbourg Cedex, France*
[b]*Institute for Advanced Study (USIAS), Université de Strasbourg, 4 rue Blaise Pascal, 67081 Strasbourg Cedex, France. E-mail: braunstein@unistra.fr, danopoulos@unistra.fr*

† Dedicated to the memory of Prof. Peter Hofmann, a dear colleague and friend who made major research advancements and contributed much to the promotion of chemistry.

‡ Electronic supplementary information (ESI) available: X-ray structure of $[Ag_2(\mathbf{L^{Ph}})_2](BF_4)_2$ and crystallographic summary table. CCDC 1445698–1445706. For ESI and crystallographic data in CIF or other electronic format see DOI: 10.1039/c6dt00275g

 This journal is © The Royal Society of Chemistry 2016

Open Access Article. Published on 11 February 2016. Downloaded on 10/20/2025 7:02:02 PM.
This article is licensed under a Creative Commons Attribution 3.0 Unported Licence.

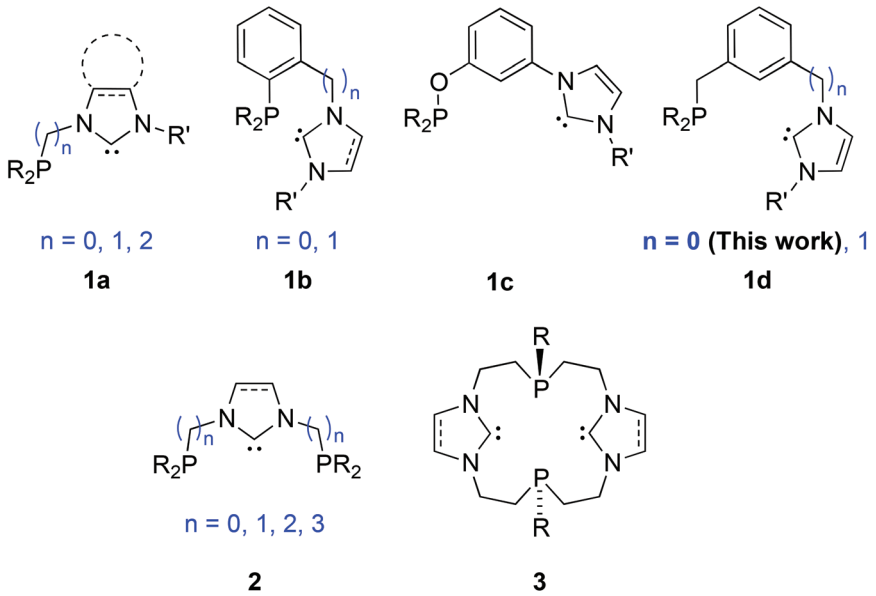


Fig. 1 Bidentate P-NHC-type (**1a–1d**), tridentate $PC^{NHC}P$ (**2**) and macrocyclic $P_2(C^{NHC})_2$ (**3**) hybrid ligands reported.

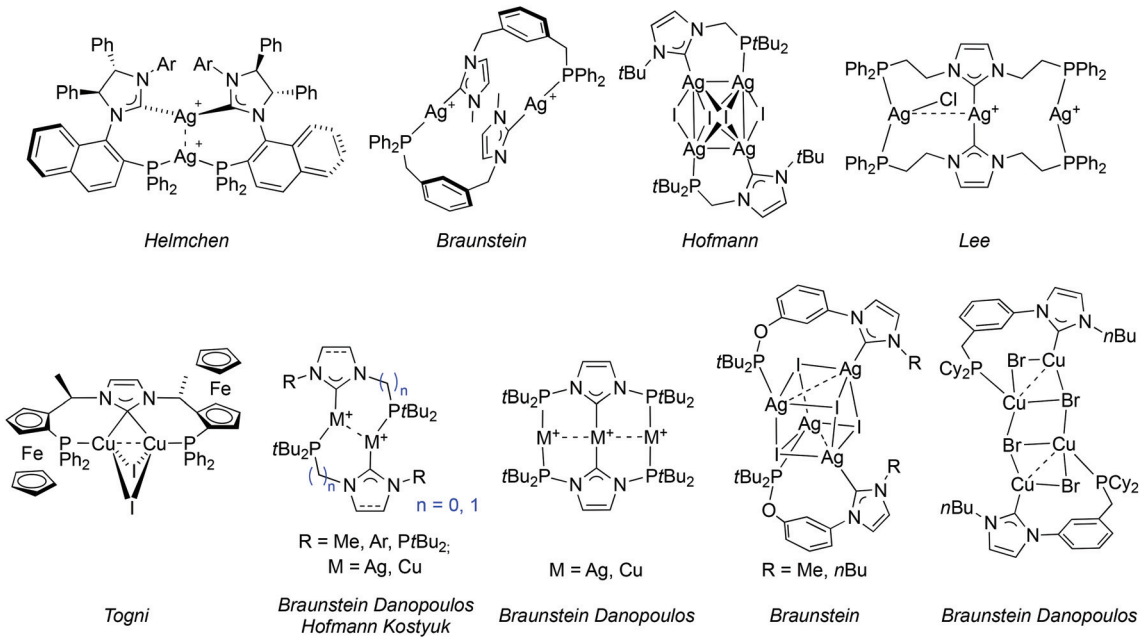


Fig. 2 Structurally characterised P–NHC-type silver(I) and copper(I) complexes reported in the literature.

complexes. Silver P–NHC complexes are usually obtained by the reaction of the corresponding imidazolium salts with $Ag_2O$,[16] or by initial formation of the free carbene ligand followed by coordination to $Ag^I$.[9c,15c] In addition to their structural diversity, they have proved to be efficient NHC transfer reagents to metals,[16] such as $Ru^{II}$,[15a,17] $Rh^I$,[11a,18] $Pd^{II}$,[6f,10g,13a] and $Au^I$;[9a,15c,19] but in rare cases the transmetallation did not proceed neatly.[10g,12c]

Interestingly, P–NHC-type copper(I) complexes are accessible by transmetallation from the corresponding $Ag^I$ complexes,[9a,12e,15c] and by other methodologies *e.g.* the coordination of the preformed free carbene to a labile $Cu^I$ precursor,[9c,10f,13b,15c] or the reaction of the imidazolium salt with precursors featuring a coordinated base (*e.g.* copper(I) acetate,[13b] mesitylcopper(I) $[Cu_5(Mes)_5]$[12e] and $[CuN(SiMe_3)_2]$).[9c]

Lastly, P–NHC gold(I) complexes are scarce (Fig. 3) but arouse increasing interest due to their attractive photophysical properties and the occurrence of metallophilic interactions in their structures.[9a,c,e,15c,19]

Extending our previous work on P-based NHC hybrid ligands,[12a,c,e] herein we report an efficient and modular access

Open Access Article. Published on 11 February 2016. Downloaded on 10/20/2025 7:02:02 PM.
This article is licensed under a Creative Commons Attribution 3.0 Unported Licence.

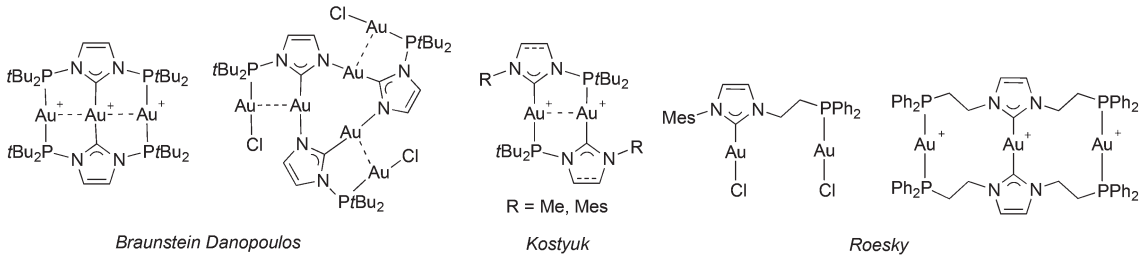


Fig. 3 Gold(I) complexes with P–NHC-type ligands reported in the literature (all since 2013).

to the $^{R}$P–NHC-type ($^{R}$P = $PCy_2$, $PtBu_2$ or $PPh_2$) ligands (see **1d** in Fig. 1) and their coinage metal complexes.

## Results and discussion

### Ligand synthesis

A synthetic strategy for the synthesis of phosphine imidazolium precursors employing silane ($SiHMeCl_2$ or $SiHCl_3$) reduction[20] of readily available phosphoryl-imidazolium salts has ample literature precedence,[6b,10a,15b,21] including attempted preparation of precursors of similar topology to those described below.[12c] This methodology requires the use of excess silane reductants and forcing conditions, usually leading to moderate yields. Therefore, an alternative, wider scope synthetic strategy was developed, that is easily adaptable to different phosphine substituents (Scheme 1).

Starting from the imidazolium–bromobenzyl derivative **A**, the air-stable phosphonium–imidazolium salts $\mathbf{L^{Cy}}$·2HBr and $\mathbf{L^{tBu}}$·2HBr were obtained by quaternisation of dicyclohexyl- and di-*tert*-butylphosphine in acetonitrile,[12e] and converted to the corresponding phosphine-imidazolium salts $\mathbf{L^{Cy}}$·HBr and $\mathbf{L^{tBu}}$·HBr by treatment with $NEt_3$. Successful single deprotonation was confirmed in the $^1$H-NMR spectra by the disappearance of the deshielded signal due to the acidic P–*H* proton ($^1J_{P-H} \approx$ 480–490 Hz). Singlets at $\delta$ 5.8 and 32.0 ppm for $\mathbf{L^{Cy}}$·HBr and $\mathbf{L^{tBu}}$·HBr, respectively, were observed in the $^{31}$P{$^1$H}-NMR spectra. Due to the relative air-sensitivity of the trialkyl-phosphine products, borane-protection of the phosphine in $\mathbf{L^{Cy}}$·HBr was carried out and yielded $\mathbf{L^{Cy}}$·HBr·$BH_3$ as an air-stable crystalline solid, the structure of which is shown in Fig. 4 (left).

When an analogous synthetic route was applied to $\mathbf{L^{Ph}}$·HBr, it failed in the step of the direct quaternisation of diphenylphosphine by **A** owing to the lower nucleophilicity of the former. To circumvent the problem, lithium diphenylphosphide ($LiPPh_2$), generated *in situ*, was reacted with **A** at low temperature (Scheme 1). Formation of $\mathbf{L^{Ph}}$·HBr was confirmed by a phosphorus resonance at $\delta$ −8.5 ppm. In the different $\mathbf{L^{R}}$ precursors, the imidazolium backbone protons usually gave

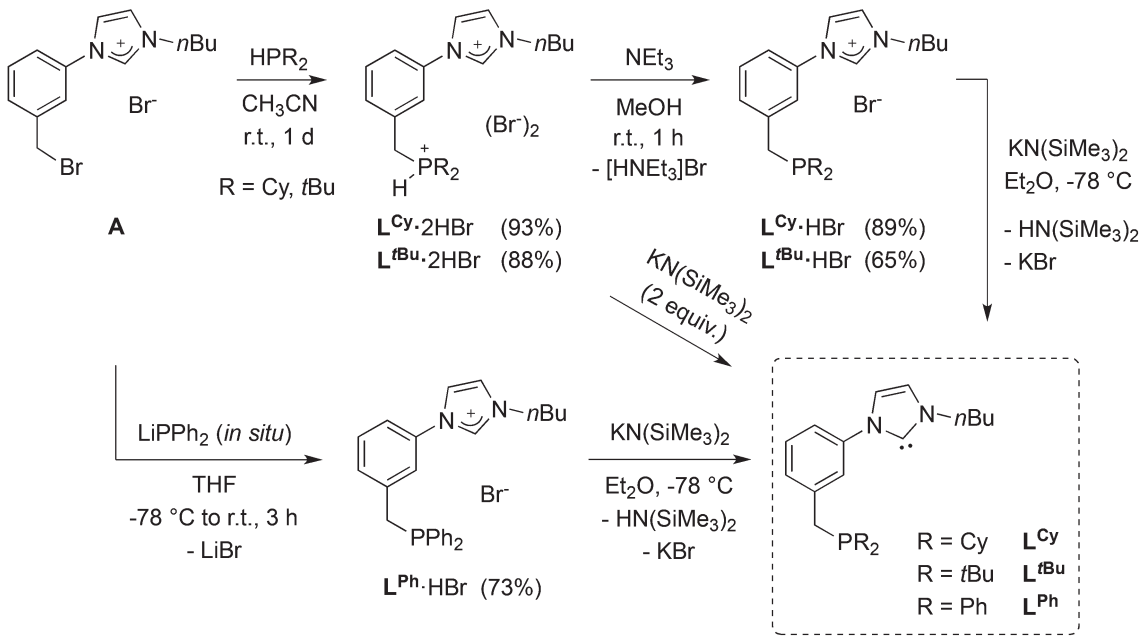


Scheme 1 Introduction of phosphine moieties to obtain hybrid P-NHC-type ligands. The synthesis of $\mathbf{L^{Cy}}$·2HBr and $\mathbf{L^{tBu}}$·2HBr has been reported in a previous communication.[12e]

Open Access Article. Published on 11 February 2016. Downloaded on 10/20/2025 7:02:02 PM.
This article is licensed under a Creative Commons Attribution 3.0 Unported Licence.

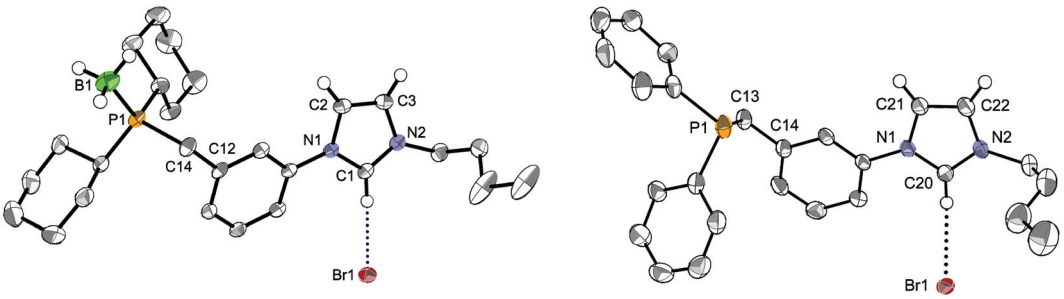


**Fig. 4** The molecular structures of the borane-protected $L^{Cy}$·HBr·$BH_3$ (left) and of $L^{Ph}$·HBr (right) with thermal ellipsoids at 40% probability. For clarity, only one disordered *n*Bu chain in $L^{Cy}$·HBr·$BH_3$ is displayed and H atoms have been omitted, except for the imidazolium and borane moieties. Selected bond distances (Å) and angles [°] for $L^{Cy}$·HBr·$BH_3$: B1–P1 1.914(3), C1–N1 1.342(3), C1–N2 1.318(3), C1H···Br1 3.511(2); N1–C1–N2 108.6(2), P1–C14–C12 117.9(2); for $L^{Ph}$·HBr: C20–N1 1.334(3), C20–N2 1.321(3), C20H···Br1 3.598(3); N1–C20–N2 108.7(2), P1–C13–C14 111.5(2).

rise in the $^1$H-NMR spectra to apparent triplets (overlapping dd, $^3J_{HH} \approx {}^4J_{HH} \approx$ 1.6–1.8 Hz), and the NC*H*N signal was observed in the range $\delta$ 11.17–11.46 ppm.

In the structure of the moderately air-stable $\mathbf{L^{Ph}}$·HBr (Fig. 4, right) the imidazolium and central aryl ring planes form an angle of 13.4° (*vs.* 22.6° for $L^{Cy}$·HBr·$BH_3$). Other bond distances and angles are unremarkable. H-bonding interactions in the solid state were evidenced by a close contact between the NC*H*N proton and the bromide anion, in addition to the high directionality of the C–H···$Br^-$ interaction.[22] Anion metathesis of $\mathbf{L^{Ph}}$·HBr and $\mathbf{L^{tBu}}$·HBr with excess $NaBF_4$ resulted in the corresponding $\mathbf{L^{Ph}}$·$HBF_4$ and $\mathbf{L^{tBu}}$·$HBF_4$ salts (see Experimental section). In their $^1$H-NMR spectra, the signal of the NC*H*N proton appeared shifted upfield ($\delta$ 9.05 and 9.18 ppm, respectively),[23] consistent with weaker hydrogen bonding compared to the bromide salts.

### Formation of the free carbenes

The free carbenes $\mathbf{L^{Cy}}$, $\mathbf{L^{tBu}}$ and $\mathbf{L^{Ph}}$ were obtained by the double deprotonation of the corresponding phosphonium–imidazolium $\mathbf{L^R}$·2HBr or the single deprotonation of phosphine–imidazolium $\mathbf{L^R}$·HBr salts with stoichiometric amounts of $KN(SiMe_3)_2$ (Scheme 1). The free carbenes were obtained in high yields (79–90%) as very air sensitive, pentane soluble, dark green oils that turned red on standing for *ca.* 30 min at room temperature. The reason for such colour change is still unclear but probably linked to thermal and/or photochemical instability, however, the products of decomposition were not identified. Despite the difficulties associated with the long-term storage and handling of the isolated $\mathbf{L^{Cy}}$, $\mathbf{L^{tBu}}$ and $\mathbf{L^{Ph}}$, unequivocal spectroscopic evidence for their identity and purity was obtained. Deprotonation and carbene formation was evidenced by the disappearance of the imidazolium signal in the $^1$H-NMR spectra of the oils and the observation of the N*C*N carbene resonance at $\delta$ 215.9–216.2 ppm.[24] Due to the difficult handling of $\mathbf{L^R}$, the synthesis of the coinage metal complexes described below is based on reactions with the imidazolium salt precursors $\mathbf{L^R}$·*n*(HBr) (*n* = 1, 2).

### Synthesis and structure of silver complexes

The availability of $\mathbf{L^R}$·HBr opened the way for a comparative study of the coordination chemistry of $\mathbf{L^R}$ as a function of R. Treatment of $\mathbf{L^{Ph}}$·HBr with 1 mole equiv. of $Ag_2O$ in acetonitrile, in the presence of 4 Å molecular sieves, afforded $[Ag_4Br_4(\mathbf{L^{Ph}})_2]$ in low yields (<50%) after recrystallization from $CH_2Cl_2/Et_2O$ (Scheme 2, route (*a*)). Upon formation of the

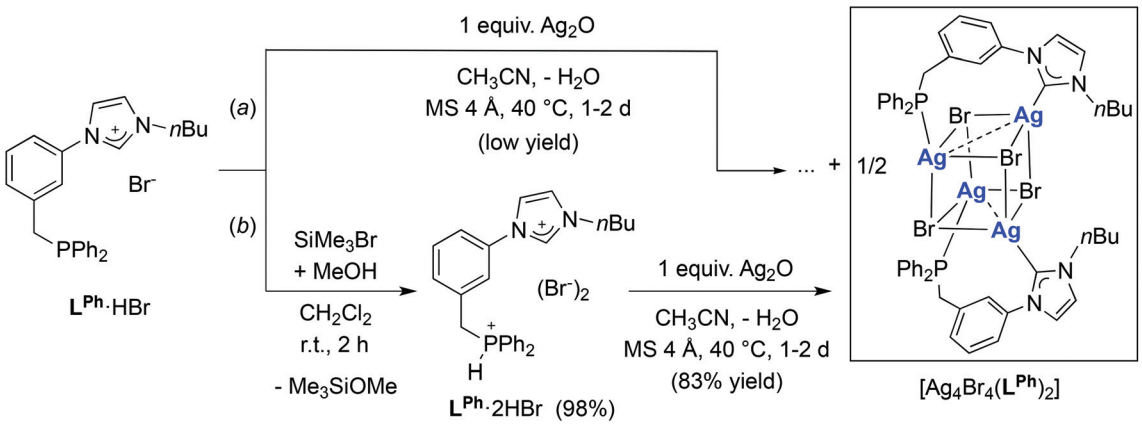


**Scheme 2** Synthesis of the silver complex $[Ag_4Br_4(\mathbf{L^{Ph}})_2]$ (yields based on $\mathbf{L^{Ph}}$).

Open Access Article. Published on 11 February 2016. Downloaded on 10/20/2025 7:02:02 PM.
This article is licensed under a Creative Commons Attribution 3.0 Unported Licence.

silver complex, the disappearance of the signal due to the acidic imidazolium proton and the downfield shift of the broad singlet at $\delta$ 3.2 ppm in the $^{1}$H-NMR and $^{31}$P-NMR spectrum, respectively, confirmed NHC formation and coordination of the P atom. The absence of P–Ag couplings ($^{107}$Ag 51.8% and $^{109}$Ag 48.2%, both $I = 1/2$) can be rationalised by a dynamic behaviour involving rapid P–Ag bond breaking/formation on the $^{31}$P-NMR timescale.[12e] In the $^{13}$C-NMR spectrum, the coordinated $C^{NHC}$ was detected as a broad singlet ($\Delta\nu_{1/2}$ = 12 Hz) at $\delta$ 186.5 ppm, in the typical range for NHC–Ag complexes.[25] The absence of $^{13}$C–$^{107/109}$Ag coupling has been reported in related NHC–AgX clusters,[12a,c,23,26] and points towards dynamic behaviour in solution[27] and a high lability of the NHC–Ag bond.[16,28]

The structure of $[Ag_4Br_4(\mathbf{L^{Ph}})_2]$ (Fig. 5) corresponds to a distorted $Ag_4Br_4$ cubane cluster with alternating vertices of the cube being occupied by Ag and Br atoms. The two bridging $\mathbf{L^{Ph}}$-κP,κ$C^{NHC}$ ligands each span the Ag···Ag diagonal of two parallel $Ag_2Br_2$ faces of the cube, forming 9-membered dimetallocycles, as observed with a closely related phosphinite–NHC ligand[12a,c] and in the structures of $[Ag_4Br_4(\mathbf{L^{R}})_2]$ (R = Cy, *t*Bu) recently reported.[12e] All bromides are capping three Ag centres. The Ag···Ag separations (3.300(1) Å and 3.400(1) Å) are shorter than the sum of the van der Waals radii for Ag (3.44 Å),[29] implying weak $d^{10}$–$d^{10}$ interactions.[30] Related $[Ag_4(halide)_4L_2]$ cubane structures have been described with L = phosphine ligands,[31] and recently obtained with bidentate ligands incorporating NHC donors (bis-NHC[23,26,32] or P–NHC-type[10g,12a,c,e] ligands). Containing non-symmetrical ligands, the observed molecular structure is chiral due to the lack of an improper axis of rotation (see Fig. 6); however, the two enantiomers are present in the asymmetric unit (related by the inversion centre of $P\bar{1}$).

Comparison of $[Ag_4Br_4(\mathbf{L^{Ph}})_2]$ with the previously reported structures of $[Ag_4Br_4(\mathbf{L^{R}})_2]$ (R = Cy, *t*Bu)[12e] reveals that the substituents on the phosphorus have little influence on the adopted motif or the metrical data. For example, with $\mathbf{L^{Ph}}$ and $\mathbf{L^{Cy}}$, the Ag–$C^{NHC}$ and Ag–P bond distances are comparable, while Ag–P is marginally longer in $[Ag_4Br_4(\mathbf{L^{tBu}})_2]$ (difference <0.040 Å). A more notable difference is in the Ag···Ag separation in each bridged face of the pseudocubane (mean Ag···Ag *ca.* 3.350 Å for $[Ag_4Br_4(\mathbf{L^{Ph}})_2]$, 3.188 Å for $[Ag_4Br_4(\mathbf{L^{Cy}})_2]$ and 3.089 Å for $[Ag_4Br_4(\mathbf{L^{tBu}})_2]$), leading to complexes with increased distortion from the idealised cubane geometry, which may be ascribed to intramolecular repulsions of the bulkier P-substituents.[33] Comparative metrical data for the different silver complexes are provided in Table 1.

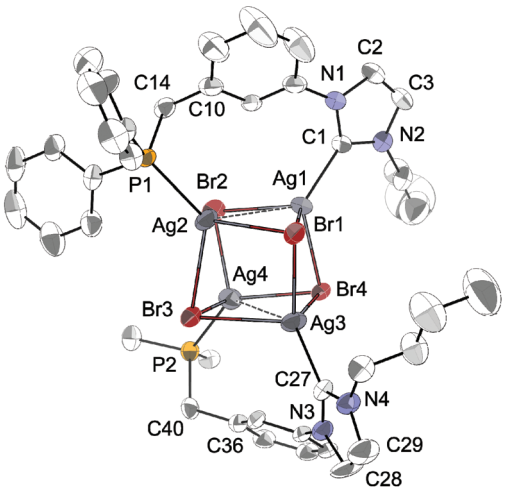


Fig. 5 The molecular structure of $[Ag_4Br_4(L^{Ph})_2]$ with thermal ellipsoids at 40% probability. For clarity, H atoms are omitted and only the *ipso* carbons of the phenyl substituents in the lower ligand are shown. Selected metrical data are given in Table 1.

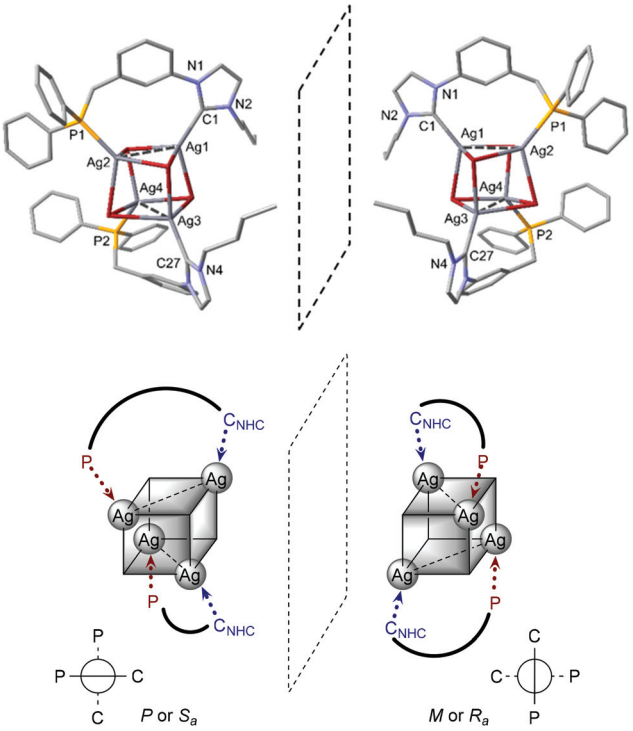


Fig. 6 Schematic representation of the two enantiomers of $[Ag_4Br_4(L^{Ph})_2]$ in the crystallographic unit cell.

In view of the similarity between $[Ag_4Br_4(\mathbf{L^{Ph}})_2]$ and $[Ag_4Br_4(\mathbf{L^{R}})_2]$ (R = Cy, *t*Bu), the latter having been obtained from the corresponding phosphonium–imidazolium salts, we reasoned that better yields of $[Ag_4Br_4(\mathbf{L^{Ph}})_2]$ should also be attainable by the reaction of $\mathbf{L^{Ph}}$·2HBr with one mole equiv. $Ag_2O$. Indeed, the reaction of $\mathbf{L^{Ph}}$·2HBr with $Ag_2O$ afforded the expected cubane complex in very good yields (>80%). It is worth noticing that the method of choice for the preparation of $\mathbf{L^{Ph}}$·2HBr consisted of protonation of $\mathbf{L^{Ph}}$·HBr by dry HBr, generated *in situ* by methanolysis of an exactly stoichiometric amount of $SiMe_3Br$ in dichloromethane under oxygen-free, controlled conditions (Scheme 2, route (b)). We also noted that the reaction of $\mathbf{L^{Ph}}$·HBr with 0.5 mole equiv. $Ag_2O$ in acetonitrile resulted in the formation of another silver complex featuring $^{1}$H NMR resonances distinct from $[Ag_4Br_4(\mathbf{L^{Ph}})_2]$, the structure of which remains elusive to date.

Open Access Article. Published on 11 February 2016. Downloaded on 10/20/2025 7:02:02 PM.
This article is licensed under a Creative Commons Attribution 3.0 Unported Licence.

**Table 1** Selected interatomic distances (Å) and angles [°] for the Ag(I) complexes $[Ag_4Br_4(L^R)_2]$ and $[Ag_2(L^R)_2](BF_4)_2$

| | $[Ag_4Br_4(L^{tBu})_2]^a$ | $[Ag_4Br_4(L^{Cy})_2]^a$ | $[Ag_4Br_4(L^{Ph})_2]$ | $[Ag_2(L^{Ph})_2](BF_4)_2{\cdot}2CH_2Cl_2$ | $[Ag_2(L^{tBu})_2](BF_4)_2{\cdot}CH_2Cl_2$ [b] |
|---|---|---|---|---|---|
| Ag1···Ag2 | 3.101(1) | 3.188(1) | 3.400(1) | 5.361(1) | 5.508(1)/5.762(1) |
| Ag3···Ag4 | 3.076(1) | 3.188(1) | 3.300(1) | | |
| Ag1···Ag3 | 3.821(1) | 3.721(1) | 3.761(1) | | |
| Ag1···Ag4 | 3.712(1) | 3.687(1) | 3.562 (1) | | |
| Ag1–Br1 | 2.688(1) | 2.880(1) | 2.949(1) | | |
| Ag1–Br2 | 3.006(1) | 2.812(1) | 2.748(1) | | |
| Ag1–Br4 | 2.895(1) | 2.708(1) | 2.721(1) | | |
| Ag2–P1 | 2.422(1) | 2.402(1) | 2.407(1) | Ag1–P2 2.386(2) | Ag1–P2 2.376(2)/2.357(2) |
| Ag4–P2 | 2.425(1) | 2.391(1) | 2.388(1) | Ag2–P1 2.376(2) | Ag2–P1 2.375(2)/2.395(2) |
| Ag1–C1 | 2.148(4) | 2.135(3) | 2.147(5) | Ag1–C1 2.113(6) | Ag1–C1 2.106(6)/2.094(6) |
| Ag3–C27 | 2.123(4) | 2.144(4) | 2.127(5) | Ag2–C27 2.108(6) | Ag2–C23 2.109(7)/2.113(7) |
| N1–C1–N2 | 103.7(4) | 103.9(3) | 103.7(5) | 104.6(1) | 104.1(5)/104.7(5) |
| N3–C27–N4 | 103.2(3) | 103.3(3) | 103.1(5) | 105.1(5) | 103.1(6)/102.5(6) |

[a] Data taken from ref. 12*e*. [b] There are two dinuclear complexes exhibiting similar metrical data in the asymmetric unit, the second set of values refers to the other molecule.

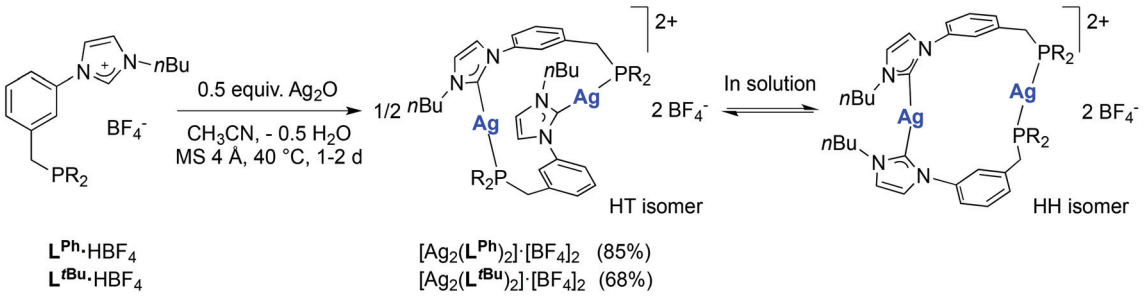


**Scheme 3** Synthesis of the silver complexes $[Ag_2(L^R)_2](BF_4)_2$ (R = Ph, *t*Bu) and 'head-to-tail' (HT)/'head-to-head' (HH) isomerisation in solution (see text). Yields are based on $L^R$.

The crucial role of halides in the formation of the cubane structures described above raised the question of the possible reaction outcome under halide-free conditions. The reaction of $L^{Ph}{\cdot}HBF_4$ with 0.5 mole equiv. of $Ag_2O$ in acetonitrile led to the complex $[Ag_2(L^{Ph})_2](BF_4)_2$ (Scheme 3). Examination of its $^1H$ and $^{31}P\{^1H\}$ NMR spectra revealed an equilibrium involving two isomers in solution. Notably, dissolution in $CD_3CN$ gave rise, in the $^{31}P\{^1H\}$ NMR spectrum, to two sets of two doublets (total 8 lines) observed at $\delta$ 21.3 (two doublets, $^1J_{P-^{107}Ag} \approx$ 500 Hz, $^1J_{P-^{109}Ag} \approx$ 580 Hz) and 11.2 ppm (two doublets, $^1J_{P-^{107}Ag} \approx$ 475 Hz, $^1J_{P-^{109}Ag} \approx$ 550 Hz) in a 1 : 1.1 ratio, respectively. Evaporation of the solvent and re-dissolution in $CD_2Cl_2$ led to a similar set of peaks but in a *ca.* 4 : 1 ratio, respectively. The reversibility of this procedure confirmed the solvent-dependency of the equilibrium. Due to limited solubility in $CD_3CN$, the $^{13}C\{^1H\}$-NMR spectrum was recorded in $CD_2Cl_2$, where only the signals for the major isomer were clearly visible. In order to gain more insight into the structures of these two isomers, crystallisations from either $CH_2Cl_2$ or $CH_3CN$ solutions were attempted. Products corresponding to $[Ag_2(L^{Ph})_2](BF_4)_2{\cdot}(solvent)_x$ were obtained from both solvents, which crystallized in different space groups as 'head-to-tail' (HT) (heteroleptic) isomers with respect to the mutual arrangement of the ligands. However, the molecular structure of the products (Fig. 7, left and Fig. S1 in ESI‡) revealed the same atom connectivity and very similar metrical data, indicating that only one and the same isomer crystallised (with a possible shift of the equilibrium between 'head-to-head' (HH) (homoleptic) and HT isomers upon crystallisation).

In the structure of $[Ag_2(L^{Ph})_2](BF_4)_2{\cdot}2CH_2Cl_2$ (Fig. 7, left), the two $L^{Ph}$ ligands bridge two Ag metal centres (Ag1···Ag2 5.361(1) Å) in a 'head-to-tail' arrangement. The $C^{NHC}$–Ag–P angles slightly deviate from linearity (C1–Ag1–P2 172.2(2)° and C27–Ag2–P1 172.7(2)°) and the two NHC rings are not parallel, their mean planes forming an angle of 12.8°. Such an arrangement has already been observed in other P–NHC-type silver complexes;[10g,12c,15b] the linear coordination geometry is also encountered in bis-NHC silver complexes with non-coordinating anions.[23,34] The Ag–$C^{NHC}$ bond distances follow trends observed for related complexes,[25a] being slightly longer in the NHC silver–halide clusters (mean *ca.* 2.137 Å)[14] than in the complexes with non-coordinating anions (mean *ca.* 2.111 Å).[14]

In order to gain insight into the solution behaviour of $[Ag_2(L^{Ph})_2](BF_4)_2$, the corresponding $[Ag_2(L^{tBu})_2](BF_4)_2$ was similarly prepared (Scheme 3). In this case too, $^1H$- and $^{31}P\{^1H\}$-NMR analysis in $CD_2Cl_2$ revealed the presence of two isomers, in a 1 : 2 ratio, the nature of which could be determined by perusal of the $^{13}C\{^1H\}$-NMR spectrum. Spectra of sufficient quality were obtained by acquisition with a cryogenically cooled probe head. A complex pattern (10 lines in total) in the

Open Access Article. Published on 11 February 2016. Downloaded on 10/20/2025 7:02:02 PM.
This article is licensed under a Creative Commons Attribution 3.0 Unported Licence.

Fig. 7 Structure of the dication in $[Ag_2(L^{Ph})_2](BF_4)_2{\cdot}2CH_2Cl_2$ (left) and of one of the two dications in $[Ag_2(L^{tBu})_2](BF_4)_2{\cdot}CH_2Cl_2$ (right), with thermal ellipsoids at 40% probability. Anions, H atoms and crystallisation solvent are omitted for clarity. C atoms for the Ph, *t*Bu and *n*Bu groups are depicted as spheres of arbitrary radii (only one C atom is displayed for these groups in the lower ligands). Selected metrical data are given in Table 1. The structure of the $[Ag_2(L^{Ph})_2](BF_4)_2$ complex, obtained by crystallisation from $CH_3CN$, is presented in the ESI.‡

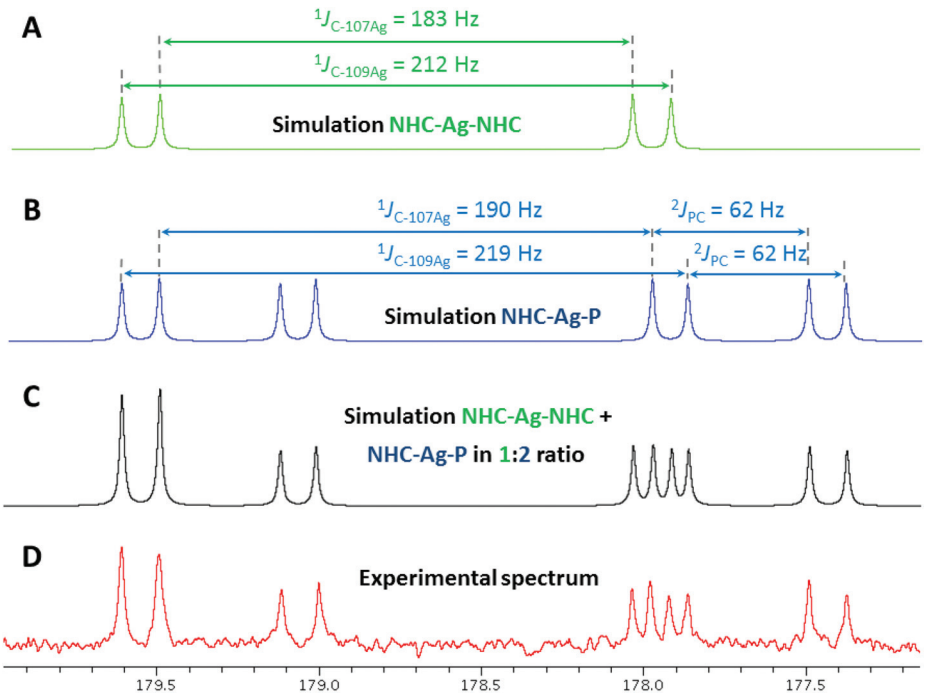


Fig. 8 Details of the $^{13}C\{^1H\}$-NMR spectrum of $[Ag_2(L^{tBu})_2](BF_4)_2$ in the $\delta$ 177–180 ppm region (D) and simulated spectra (TOPSPIN-DAISY module) of the homoleptic (HH) NHC–Ag–NHC isomer (A), the heteroleptic (HT) NHC–Ag–P isomer (B) and both the HH and HT isomers in a 1 : 2 ratio (C). Spectrum recorded in $CD_2Cl_2$ at 125.77 MHz and 298 K with a cryogenically cooled probe head; accumulation of 1024 scans.

region $\delta$ 180–177 ppm, corresponding to the $C^{NHC}$–Ag signals was successfully simulated, revealing two different $C^{NHC}$–Ag environments associated with the different isomers (Fig. 8): the two doublets centred at $\delta$ 178.8 ppm ($^1J_{C-107Ag}$ = 183 Hz, $^1J_{C-109Ag}$ = 212 Hz) were attributed to an isomer with homoleptic $Ag^I$ centres and symmetrical NHC–Ag–NHC coordination (HH isomer), while two doublets of doublets at $\delta$ 178.5 ppm ($^1J_{C-107Ag}$ = 190 Hz, $^1J_{C-109Ag}$ = 219 Hz, $^2J_{P-Ag-C}$ = 62 Hz) were assigned to the second and major isomer, with heteroleptic NHC–Ag–P connectivity (HT isomer). Further indication of the nature of the former isomer was obtained from the observation in $^{13}$C-NMR of 'virtual' triplets of the $X_nAA'X'_n$ (X = X′ = C, A = A′ = P) spin system involving the carbon atoms directly bound to phosphorus, resulting from a strong $^2J_{PAgP}$ coupling between *trans*-coordinated P donors.[35] Interestingly, for all $[Ag_2(L^R)_2](BF_4)_2$ (R = Ph, *t*Bu) complexes, the $^1$H-NMR signals for the NHC backbone protons were detected as apparent triplets, likely due to $^4J_{HAg}$ and $^3J_{HH}$ coupling constants falling in the same range.[36]

An X-ray diffraction study of $[Ag_2(L^{tBu})_2](BF_4)_2$ also revealed a 'head-to-tail' coordination of the bidentate ligand (Fig. 7, right), with two crystallographically independent but very similar dinuclear complexes in the unit cell (Table 1). The bond distances and angles in $[Ag_2(L^R)_2]^{2+}$ for R = Ph and *t*Bu are very close or within experimental error, showing that the nature of the P donor group has only little influence on the solid state structure.

Interestingly, Hofmann and co-workers recently reported the formation of P–NHC-type 'head-to-head' and 'head-to-tail'

 This journal is © The Royal Society of Chemistry 2016

Open Access Article. Published on 11 February 2016. Downloaded on 10/20/2025 7:02:02 PM.
This article is licensed under a Creative Commons Attribution 3.0 Unported Licence.

copper(I) complexes.[10f] Depending on the nature of NHC wingtip, either the homoleptic or the heteroleptic isomer was isolated. Mutual '*trans*-coordination' of the NHC and P donors, electronically disfavoured,[37] was rationalised by minimisation of the steric repulsion in the 'head-to-head' complex. Yet for these complexes, no 'head-to-head'/'head-to-tail' isomerisation was detected in different NMR solvents.

### Synthesis and structure of dinuclear copper(I) complexes

We have already reported the synthesis of tetranuclear, ladder-type P–NHC-type $Cu^I$ complexes by transmetallation from $[Ag_4Br_4(\mathbf{L^R})_2]$ or by reaction of the phosphonium–imidazolium $\mathbf{L^R}$·2HBr salts with mesitylcopper(I) $[Cu_5(Mes)_5]$,[12e] which has been used before to form $Cu^I$ NHC complexes from imidazolium salts.[38] The coordination chemistry of the $\mathbf{L^R}$ ligands with $Cu^I$ was further investigated by using the monoprotic proligands $\mathbf{L^R}$·HBr.

Reaction of $\mathbf{L^R}$·HBr (R = Ph, *t*Bu, Cy) with $[Cu_5(Mes)_5]$ resulted in the formation of the corresponding $[Cu_2Br_2(\mathbf{L^R})_2]$ complexes in good yields (Scheme 4). Completion of the reaction was evidenced by $^1$H NMR spectroscopy (*i.e.* disappearance of the imidazolium NC*H*N signal). For all three $Cu^I$ complexes, the $^{31}P\{^1H\}$-NMR spectra revealed a singlet assignable to the coordinated P donor, only slightly shifted from the position observed in the starting $\mathbf{L^R}$·HBr. In the $^{13}C\{^1H\}$-NMR spectra, the $Cu^I$–$C^{NHC}$ resonance was detected in the region $\delta$ 183–186 ppm, typical for $Cu^I$–NHCs.[25b] The $C^{NHC}$ signal was observed as a doublet ($^2J_{PC} \approx 46$–47 Hz) for the dialkyl phosphine derivatives or as a broad signal for $[Cu_2Br_2(\mathbf{L^{Ph}})_2]$, possibly due to a different rate of fluxionality of the $C^{NHC}$–Cu bonds in these two complexes. In the $^1$H-NMR spectrum of $[Cu_2Br_2(\mathbf{L^{tBu}})_2]$, the line-shape of the signals for the methylene protons was field-dependent, pointing towards a dynamic process in solution.

The structures of $[Cu_2Br_2(\mathbf{L^{Cy}})_2]$ and $[Cu_2Br_2(\mathbf{L^{tBu}})_2]\cdot 2CH_2Cl_2$ were determined crystallographically and are depicted in Fig. 9. Both complexes crystallised as dimers with two $\mathbf{L^R}$ ligands bridging the two copper centres, reminiscent of the coordination behaviour of the ligands in $[Ag_2(\mathbf{L^R})_2](BF_4)_2$. Both structures present a 'head-to-tail' arrangement for the NHC and P donors. The three-coordinate Cu centres adopt a distorted planar T-shaped coordination geometry, the third donor being a bromide. The Cu–$C^{NHC}$ distances, from 1.938(6) to 1.960(6) Å, and the Cu–P bond lengths lie within the range reported for related complexes.[10f,39] The large separation between the two $Cu^I$ centres (from 6.836(1) to 7.138(1) Å) can be traced to the large 1,3-phenylene spacer linking the NHC and phosphine donors.

In order to study further the dynamic behaviour of the $Cu^I$ complexes in solution, we undertook a variable temperature (VT) $^1$H-NMR study of $[Cu_2Br_2(\mathbf{L^{tBu}})_2]$ in $CD_2Cl_2$ prompted by its relatively simple line-shape compared to the $\mathbf{L^{Ph}}$ and $\mathbf{L^{Cy}}$

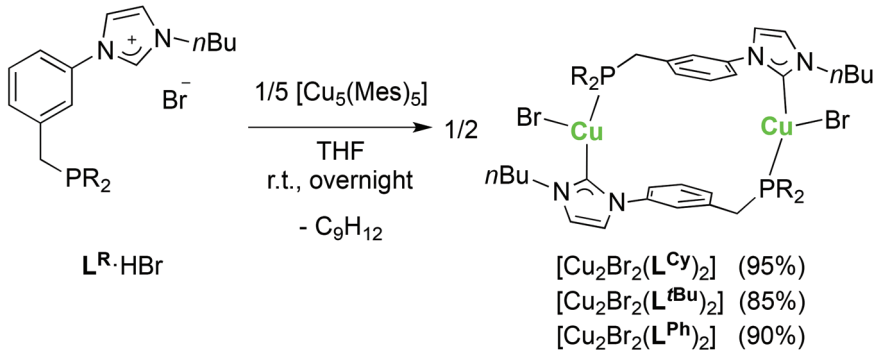


**Scheme 4** Synthesis of the dinuclear copper(I) complexes $[Cu_2Br_2(\mathbf{L^R})_2]$. Yields are based on $\mathbf{L^R}$.

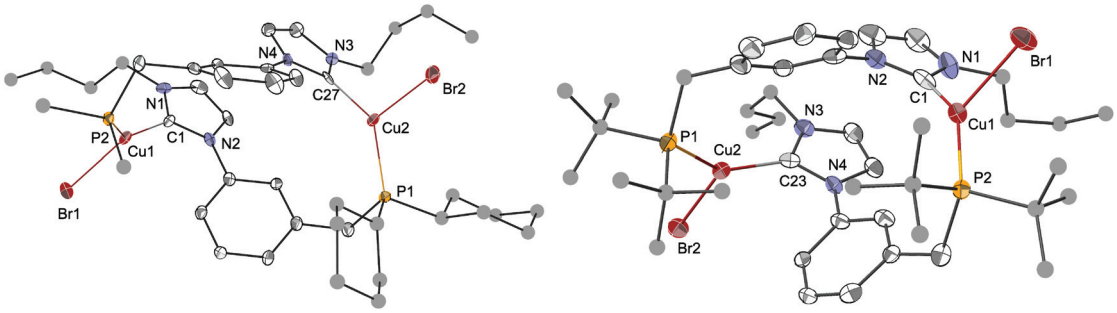


**Fig. 9** The molecular structures of $[Cu_2Br_2(\mathbf{L^{Cy}})_2]$ (left) and $[Cu_2Br_2(\mathbf{L^{tBu}})_2]\cdot 2CH_2Cl_2$ (right) with thermal ellipsoids at 40% probability. In $[Cu_2Br_2(\mathbf{L^{Cy}})_2]$ only one Cy carbon and one disordered position for the *n*Bu chain are shown for clarity. C atoms for the *n*Bu, Cy and *t*Bu groups are depicted as spheres of arbitrary radii. H atoms and crystallisation solvents have been removed for clarity. Selected metrical data are given in Table 2.

Open Access Article. Published on 11 February 2016. Downloaded on 10/20/2025 7:02:02 PM.
This article is licensed under a Creative Commons Attribution 3.0 Unported Licence.

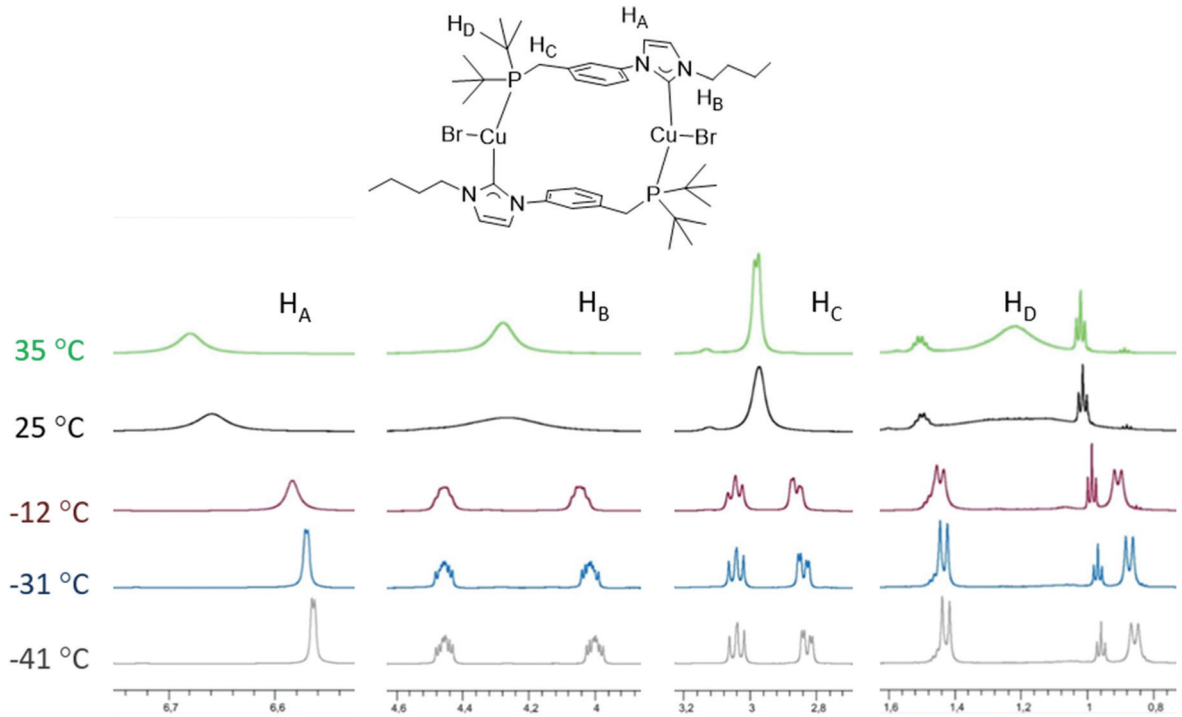


Fig. 10 VT $^1$H NMR (600 MHz) spectra of $[Cu_2Br_2(L^{tBu})_2]$ in $CD_2Cl_2$ at temperatures from −41 to +35 °C.

analogues (Fig. 10). At room temperature, very broad signals were observed at 600 MHz for the various protons, suggesting possible coalescence. Upon cooling to −41 °C, two sharp doublets at $\delta$ 1.43 and 0.86 ppm (9 H each) assignable to the *t*Bu groups on P indicated a static structure ($H_D$). At this temperature, the signal of the methylene protons ($H_C$) was split into two complex multiplets, due to the geminal $^2J_{HH}$ and $^2J_{PH}$ coupling in an ABX (A = B = H, X = P) spin system. Interestingly, the $NCH_2$ protons ($H_B$) of the NHC wingtip also appeared as diastereotopic. The backbone $H_A$ proton, closer to the aryl spacer, gives rise to a doublet at this temperature owing to $^3J_{HH}$ coupling. For comparison, at 35 °C, one broad singlet (18 H) was assignable to the *t*Bu groups on P and a doublet was observed for the methylene protons ($H_C$) in accordance with a relatively fast exchange of their positions on the NMR time scale. The spectral characteristics at lower temperature are in agreement with the solid-state structure being retained in solution. The dynamic behaviour at higher temperatures may have diverse origins, *i.e.* conformational changes in the dimeric structure involving flipping of the phenylene linker and/or the reversible formation of 'head-to-head' coordinated dimers by ligand (hemi)lability. The activation barrier corresponding to the fluxional behaviour of the *t*Bu groups was found to be $\Delta G^{\ddagger}$ = 56.5 ± 1.0 kJ mol$^{-1}$. Based on the current data there is no preference for any of the above explanations. The latter hypothesis is however less likely since only one singlet is observed in the $^{31}P\{^1H\}$-NMR spectrum at room temperature. Recent work involving ligands with NHC and P donors held together by a $CH_2$ linker ascribed stereo-isomerisations at the Cu centre to fluxionality.[10f]

In contrast, the reaction of $[Cu_5(Mes)_5]$ with the phosphonium–imidazolium $\mathbf{L^R}$·2HBr, or the transmetallation of the corresponding $[Ag_4Br_4(\mathbf{L^R})_2]$ cubanes with 4 mole equiv. of $[CuBr{\cdot}SMe_2]$ (R = Cy, *t*Bu) gave rise to the tetranuclear clusters $[Cu_4Br_4(\mathbf{L^R})_2]$.[12e] Metrical data regarding the di- and tetranuclear $Cu^I$ complexes are reported in Table 2.

The longer Cu–$C^{NHC}$ and Cu–P bond distances in the $[Cu_2Br_2(\mathbf{L^R})_2]$ complexes (mean distances *ca.* 1.948 and 2.228 Å, respectively) in comparison to the $[Cu_4Br_4(\mathbf{L^{Cy}})_2]$ cluster (1.903(5) Å and 2.211(2) Å) probably originate from the competition between mutually *trans* strong P and NHC σ-donors.

Table 2 Selected interatomic distances (Å) and angles [°] for the copper complexes $[Cu_2Br_2(\mathbf{L^R})_2]$ (R = Cy, *t*Bu) and comparison with $[Cu_4Br_4(\mathbf{L^{Cy}})_2]^a$

| | $[Cu_2Br_2(L^{tBu})_2]$ | $[Cu_2Br_2(L^{Cy})_2]^b$ | $[Cu_4Br_4(L^{Cy})_2]^a$ |
|---|---|---|---|
| Cu1···Cu2 | 6.899(1) | 7.138(1)/6.836(1) | 2.790(1) |
| Cu1–Br1 | 2.497(1) | 2.453(1)/2.493(1) | 2.442(1) |
| Cu2–Br2 | 2.483(1) | 2.438(1)/2.493(1) | 2.503(1) |
| Cu1–P2 | 2.231(2) | 2.222(2)/2.230(2) | |
| Cu2–P1 | 2.237(2) | 2.217(2)/2.230(2) | 2.211(2) |
| Cu1–C1 | 1.960(6) | 1.952(6)/1.947(6) | 1.903(5) |
| Cu2–C23/C27 | 1.938(6) | 1.943(6)/1.947(6) | |
| P2–Cu1–Br1 | 114.8(1) | 109.7(1)/142.4(2) | |
| P2–Cu1–C1 | 145.1(2) | 137.9(2)/107.5(1) | |
| C1–Cu1–Br1 | 100.0(2) | 112.2(2)/110.1(2) | |
| $\sum_{angles}$ around Cu1 | 359.9 | 359.8/360.0 | |
| $\sum_{angles}$ around Cu2 | 360.0 | 360.0/360.0 | |

[a] Data taken from ref. 12e. [b] There are two dinuclear complexes exhibiting similar metrical data in the asymmetric unit, the second set of values refers to the other molecule.

 This journal is © The Royal Society of Chemistry 2016

Open Access Article. Published on 11 February 2016. Downloaded on 10/20/2025 7:02:02 PM.
This article is licensed under a Creative Commons Attribution 3.0 Unported Licence.

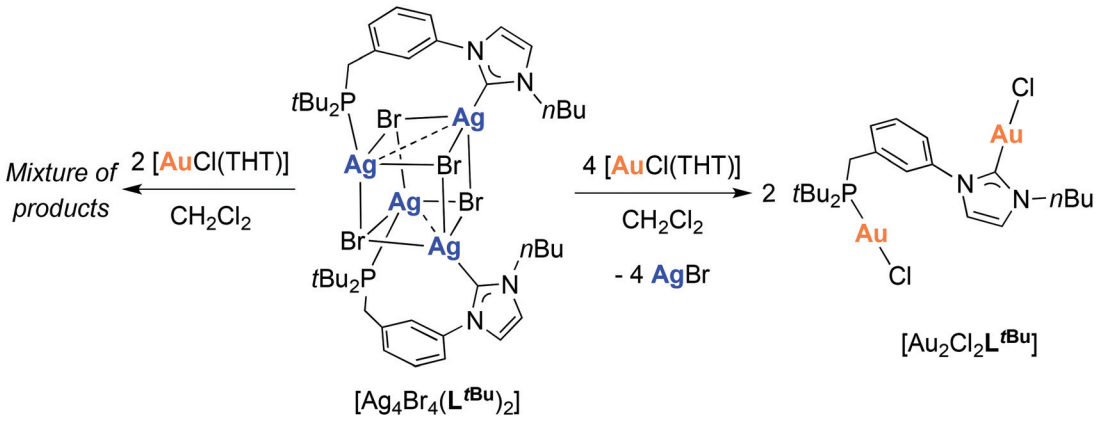


Scheme 5 Transmetallation from $[Ag_4Br_4(\mathbf{L}^{t\mathbf{Bu}})_2]$[12e] to obtain the dinuclear $[Au_2Cl_2\mathbf{L}^{t\mathbf{Bu}}]$ complex.

### Synthesis and structure of a dinuclear gold(I) complex

Since transmetallation of the silver cubane $[Ag_4Br_4(\mathbf{L}^{t\mathbf{Bu}})_2]$ with $Cu^I$ always led to tetranuclear complexes,[12e] we wondered what would happen with $Au^I$. Reaction of $[Ag_4Br_4(\mathbf{L}^{t\mathbf{Bu}})_2]$ with 4 mole equiv. of [AuCl(THT)] led to the homodinuclear gold complex $[Au_2Cl_2\mathbf{L}^{t\mathbf{Bu}}]$ (Scheme 5). $^{13}C\{^1H\}$-NMR spectral analysis supported the NHC transmetallation as a downfield singlet was detected at $\delta$ 170.3 ppm, in a range typical for $Au^I$–$C^{NHC}$ functionalities.[40] A singlet at $\delta$ 79.0 ppm in the $^{31}P\{^1H\}$-NMR spectrum also confirmed concomitant phosphine transfer to gold. However, a minor peak was observed at $\delta$ 80.1 ppm and ascribed to analogous complexes originating from partial halide scrambling (Cl/Br); this was also supported by elemental analysis (*cf.* Experimental section).

The structure of $[Au_2Cl_2\mathbf{L}^{t\mathbf{Bu}}]$ (Fig. 11) revealed an approximate linear coordination of the $Au^I$ centres (P–Au–Cl: 177.7(1)° and $C^{NHC}$–Au–Cl: 176.4(2)°), common for NHC gold(I) complexes. The Au–$C^{NHC}$ (1.985(5) Å) and Au–P (2.239(1) Å) bond distances are in the expected range.[19,40] Contrary to a recent report by Roesky and co-workers on related P–NHC-type gold(I) complexes (Fig. 3) obtained by transmetallation from the silver analogues,[19] no intra- or inter-molecular Au–Au interactions were observed in the solid state for $[Au_2Cl_2\mathbf{L}^{t\mathbf{Bu}}]$.

Attempts to synthesise heterobimetallic silver–gold complexes proved unsuccessful, as the reaction of $[Ag_4Br_4(\mathbf{L}^{t\mathbf{Bu}})_2]$ with 2 mole equiv. of [AuCl(THT)] led to a mixture of products containing $[Au_2Cl_2\mathbf{L}^{t\mathbf{Bu}}]$.

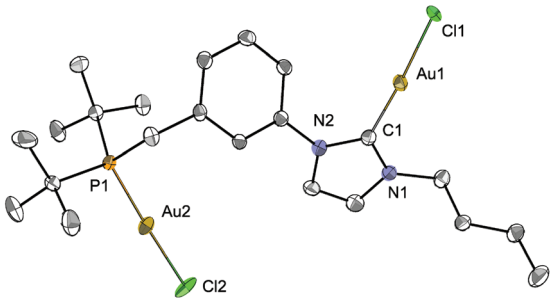


Fig. 11 The molecular structure of $[Au_2Cl_2\mathbf{L}^{t\mathbf{Bu}}]$ with thermal ellipsoids at 40% probability. Hydrogen atoms are omitted for clarity. Selected bond distances (Å) and angles [°]: Au1–Cl1 2.323(1), Au2–Cl2 2.325(1), Au1–C1 1.985(5), Au2–P1 2.239(1); C1–Au1–Cl1 176.39(15), P1–Au2–Cl2 177.69(5), N1–C1–N2 104.3(4).

## Conclusion

The rational synthesis of a range of hybrid P–NHC-type (pro-)ligands with systematically varied substitution at P, provided insight into their coordination chemistry with coinage metals. The main features observed can be summarised as follows: (i) in all cases studied, the ligands bridge two metal centres, irrespective of the type of phosphine donor; (ii) in the presence of $Br^-$, all silver complexes isolated adopt structures based on the $[Ag_4Br_4(\mathbf{L}^{\mathbf{R}})_2]$ motif comprising a distorted $Ag_4Br_4$ cubane core, bridging $\mathbf{L}^{\mathbf{R}}$ ligands and weak metallophilic interactions; (iii) in the presence of the non-coordinating $BF_4^-$, $[Ag_2(\mathbf{L}^{\mathbf{R}})_2](BF_4)_2$ complexes were obtained with bridging 'head-to-tail' ligand arrangement in the solid state and 'head-to-tail'/'head-to-head' isomerisation in solution; (iv) the nature of the R substituent on the P end does not impact the structures of the Ag complexes characterised, but seems to influence the rates of dynamic processes in solution, presumably due to competition of electronic and steric factors of the P donor. The relative lability of the two types of donor ends in P–NHC-type hybrid ligands has been inferred from the nature of products obtained from the reaction of $[Ag_4Br_4(\mathbf{L}^{\mathbf{R}})_2]$ with $[Ir(COD)(\mu\text{-}Cl)]_2$;[12e] (v) dinuclear $[Cu_2Br_2(\mathbf{L}^{\mathbf{R}})_2]$ complexes with bridging ligands were easily accessible from $\mathbf{L}^{\mathbf{R}}$·HBr and $[Cu_5(Mes)_5]$ and are also non-rigid in solution; (vi) transmetallation of $[Ag_4Br_4(\mathbf{L}^{\mathbf{R}})_2]$ with [AuCl(THT)] results in transfer of both donor groups of the hybrid P–NHC-type ligands, leading to the dinuclear $[Au_2Cl_2\mathbf{L}^{t\mathbf{Bu}}]$ complex.

Guided by the synthesis of non-symmetrical (pro)ligands and through the understanding of their emerging coordination chemistry, ligand alterations may be targeted to favour chelating and/or pincer rather than bridging coordination

Open Access Article. Published on 11 February 2016. Downloaded on 10/20/2025 7:02:02 PM.
This article is licensed under a Creative Commons Attribution 3.0 Unported Licence.

behaviour. In addition, the pre-organized tethering of the two types of strong σ-donors on the same skeleton (as on $\mathbf{L^R}$) will provide insight into the donor competition behaviour that may lead to (hemi)labile or stable complexes with catalytic potential.[12e]

## Experimental section

### General methods

All air- and moisture-sensitive manipulations were performed under dry argon atmosphere using standard Schlenk techniques. THF and $Et_2O$ were dried by refluxing over sodium/benzophenone ketyl and distilled under an argon atmosphere prior use. Methanol and ethanol were refluxed over $CaH_2$, distilled under an argon atmosphere and stored over 3 Å molecular sieves. Other solvents (pentane, $CH_2Cl_2$, toluene and acetonitrile) were dried by passing through columns of activated alumina and subsequently purged with argon. $C_6D_6$ and toluene-$d_8$ were distilled over KH; other deuterated solvents were dried over 4 Å ($CD_2Cl_2$ and $CDCl_3$) or 3 Å ($CD_3OD$) molecular sieves, degassed by freeze–pump–thaw cycles, and stored under argon. Mesityl copper(I)[41] and [AuCl(THT)][42] were prepared according to literature methods and all other chemicals were obtained from commercial sources and used without further purification. The synthesis of 1-(3-(bromomethyl) phenyl)-3-butyl-1*H*-imidazol-3-ium bromide (**A**), $\mathbf{L^{Cy}}$·2HBr, $\mathbf{L^{tBu}}$·2HBr, $[Ag_4Br_4(\mathbf{L^{Cy}})_2]$, $[Ag_4Br_4(\mathbf{L^{tBu}})_2]$ and $[Cu_4Br_4(\mathbf{L^{Cy}})_2]$ has already been reported in a recent communication.[12e]

NMR spectra were recorded on Bruker spectrometers (AVANCE I – 300 MHz, AVANCE III – 400 MHz, AVANCE III – 600 MHz or AVANCE I – 500 MHz equipped with a cryogenic probe). Downfield shifts are reported in ppm as positive and referenced using signals of the residual protio solvent ($^1$H), the solvent ($^{13}$C) or externally ($^{31}$P, $^{11}$B). All NMR spectra were measured at 298 K, unless otherwise specified. The multiplicity of the signals is indicated as s = singlet, d = doublet, t = triplet, q = quartet, quint = quintet, sext = sextet, m = multiplet and br = broad. Unequivocal determination of $^nJ_{PC}$ coupling constants in ambiguous cases was carried out by recording the $^{13}C\{^1H\}$-NMR spectra on two different field spectrometers. Assignments (Fig. 12) were determined either on the basis of unambiguous chemical shifts, coupling patterns and $^{13}$C-DEPT experiments or 2D correlations ($^1$H–$^1$H COSY, $^1$H–$^{13}$C HSQC, $^1$H–$^{13}$C HMBC). Spin-simulation was carried out using the DAISY module of the Topspin 2.1 software (BRUKER).

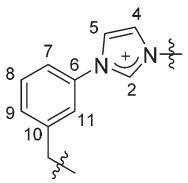


Fig. 12 Atom numbering used for the assignment of the NMR resonances.

Elemental analyses were performed by the "Service de microanalyses", Université de Strasbourg. Electrospray mass spectra (ESI-MS) were recorded on a microTOF (Bruker Daltonics, Bremen, Germany) instrument using nitrogen as drying agent and nebulizing gas.

**Synthesis of 3-butyl-1-(3-((dicyclohexylphosphino)methyl)-phenyl)-1*H*-imidazol-3-ium bromide ($\mathbf{L^{Cy}}$·HBr).** To a solution of $\mathbf{L^{Cy}}$·2HBr (5.51 g, 9.63 mmol) in degassed methanol (15 mL) was added under argon a solution of $NEt_3$ (6.5 mL, 4.88 g, 48 mmol) in methanol (5 mL). After the resulting solution was stirred at r.t. for 1 h, all the volatiles were evaporated under reduced pressure. The oily residue was redissolved in $CH_2Cl_2$ and the solution was extracted three times with degassed water to remove the triethylammonium salt. The organic phase was dried over anhydrous $MgSO_4$ and concentrated under reduced pressure. Addition of a mixture of $Et_2O$ and pentane precipitated $\mathbf{L^{Cy}}$·HBr as a white powder that was isolated by filtration and dried under vacuum. Yield: 4.20 g (8.55 mmol), 89%. Anal. Calcd for $C_{26}H_{40}BrN_2P$ (491.49): C, 63.54; H, 8.20; N, 5.70. Found: C, 63.04; H, 8.07; N, 5.64. $^1$H NMR (500.13 MHz, $CD_2Cl_2$): $\delta$ 11.19 (t, $^4J_{HH}$ = 1.6 Hz, 1H, C*H*$_{imid.}$ H2), 7.67 (d, $^3J_{HH}$ = 7.8 Hz, 1H, C*H*$_{arom.}$ H7/H9), 7.64 (t, $^3J_{HH}$ = $^4J_{HH}$ = 1.7 Hz, 1H, C*H*$_{imid.}$ H4/H5), 7.60 (br s, 1H, C*H*$_{arom.}$ H11), 7.57 (t, $^3J_{HH}$ = $^4J_{HH}$ = 1.7 Hz, 1H, C*H*$_{imid.}$ H5/H4), 7.47 (t, $^3J_{HH}$ = 7.8 Hz, 1H, C*H*$_{arom.}$ H8), 7.42 (d, $^3J_{HH}$ = 7.8 Hz, 1H, C*H*$_{arom.}$ H9/H7), 4.57 (t, $^3J_{HH}$ = 7.4 Hz, 2H, NC*H*$_2$), 2.90 (br s, 2H, C*H*$_2$P), 1.98 (quint, $^3J_{HH}$ = 7.5 Hz, 2H, NCH$_2$C*H*$_2$), 1.81–1.63 (m, 10H, Cy), 1.63–1.54 (m, 2H, Cy), 1.44 (sext, $^3J_{HH}$ = 7.5 Hz, 2H, NCH$_2$CH$_2$C*H*$_2$), 1.31–1.06 (m, 10H, Cy), 0.99 (t, $^3J_{HH}$ = 7.4 Hz, 3H, C*H*$_3$). $^{13}C\{^1H\}$ NMR (125.77 MHz, $CD_2Cl_2$): $\delta$ 144.8 (d, $^2J_{PC}$ = 10.0 Hz, *C*$_{arom.}$ C10), 136.7 (*C*H$_{imid.}$ C2), 134.9 (*C*$_{arom.}$ C6), 131.5 (d, $J_{PC}$ = 7.1 Hz, *C*H$_{arom.}$), 130.6 (*C*H$_{arom.}$), 122.9 (*C*H$_{arom.}$), 122.4 (d, $J_{PC}$ = 8.2 Hz, *C*H$_{arom}$), 120.7 (*C*H$_{arom.}$), 119.4 (*C*H$_{arom.}$), 50.4 (N*C*H$_2$), 33.9 (d, $^1J_{PC}$ = 14.9 Hz, *C*H$_{Cy}$), 32.6 (NCH$_2$*C*H$_2$), 30.2 (d, $J_{PC}$ = 13.1 Hz, *C*H$_{2\ Cy}$), 29.7 (d, $J_{PC}$ = 9.1 Hz, *C*H$_{2\ Cy}$), 29.3 (d, $^1J_{PC}$ = 21.7 Hz, *C*H$_2$P), 27.64 (d, $J_{PC}$ = 10.8 Hz, *C*H$_{2\ Cy}$), 27.56 (d, $J_{PC}$ = 8.3 Hz, *C*H$_{2\ Cy}$), 26.8 (s, *C*H$_{2\ Cy}$), 19.8 (NCH$_2$CH$_2$*C*H$_2$), 13.7 (*C*H$_3$). $^{31}P\{^1H\}$ NMR (161.98 MHz, $CD_2Cl_2$): $\delta$ 5.8.

**Synthesis of 3-butyl-1-(3-((dicyclohexylphosphino)methyl)-phenyl)-1*H*-imidazol-3-ium bromide borane adduct ($\mathbf{L^{Cy}}$·HBr·BH$_3$).** To a suspension of $\mathbf{L^{Cy}}$·HBr (0.50 g, 1.0 mmol) in THF precooled at −10 °C was added dropwise $BH_3{\cdot}SMe_2$ (0.55 mL of a 2.0 M THF solution, 1.1 mmol). The reaction mixture was allowed to reach r.t. and stirred for 2 h. All volatiles were evaporated under reduced pressure and the resulting white powder was washed with $Et_2O$ and dried under vacuum. Yield: 0.50 g (0.99 mmol), 99%. Single crystals suitable for X-ray diffraction were obtained by slow diffusion of $Et_2O$ in a $CH_2Cl_2$ solution of $\mathbf{L^{Cy}}$·HBr·BH$_3$. Anal. Calcd for $C_{26}H_{43}BBrN_2P$ (505.33): C, 61.80; H, 8.58; N, 5.54. Found: C, 61.50; H, 8.50; N, 5.52. $^1$H NMR (300.13 MHz, $CDCl_3$): $\delta$ 11.42 (t, $^4J_{HH}$ = 1.7 Hz, 1H, C*H*$_{imid.}$ H2), 7.91 (dm, $^3J_{HH}$ = 8.0 Hz, 1H, C*H*$_{arom.}$ H7/H9), 7.80 (q, $^4J_{HH}$ = $^4J_{PH}$ = 1.8 Hz, 1H, C*H*$_{arom.}$ H11), 7.69 (t, $^3J_{HH}$ = $^4J_{HH}$ = 1.8 Hz, 1H, C*H*$_{imid.}$ H4/H5), 7.52 (t, $^3J_{HH}$ = 7.9 Hz, 1H, C*H*$_{arom.}$ H8), 7.37 (t, $^3J_{HH}$ = $^4J_{HH}$ = 1.8 Hz, 1H, C*H*$_{imid.}$ H5/H4),

 This journal is © The Royal Society of Chemistry 2016

Open Access Article. Published on 11 February 2016. Downloaded on 10/20/2025 7:02:02 PM.
This article is licensed under a Creative Commons Attribution 3.0 Unported Licence.

7.36 (br overlapping d, $^3J_{HH} \approx 8.0$ Hz, 1H, C*H*$_{arom.}$ H9/H7), 4.59 (t, $^3J_{HH} = 7.4$ Hz, 2H, NC*H*$_2$), 3.13 (d, $^2J_{PH} = 12.1$ Hz, 2H, C*H*$_2$P), 1.99 (quint, $^3J_{HH} = 7.5$ Hz, 2H, NCH$_2$C*H*$_2$), 1.94–1.63 (m, 12H, Cy), 1.46 (sext, $^3J_{HH} = 7.5$ Hz, 2H, NCH$_2$CH$_2$C*H*$_2$), 1.40–1.12 (m, 10H, Cy), 1.00 (t, $^3J_{HH} = 7.3$ Hz, 3H, C*H*$_3$), 0.41 (br d, $^1J_{BH} \approx$ 90–100 Hz, 3H, BH$_3$). $^{13}$C{$^1$H} NMR (75.48 MHz, CDCl$_3$): $\delta$ 137.0 (d, $J_{PC} = 3.5$ Hz), 136.4, 134.3 (d, $J_{PC} = 2.4$ Hz), 131.5 (d, $J_{PC} = 4.5$ Hz), 130.7, 123.2 (d, $J_{PC} = 3.6$ Hz), 122.6, 120.52, 120.48, 50.4 (N*C*H$_2$), 32.4 (NCH$_2$*C*H$_2$), 32.1 (d, $^1J_{PC} = 30.9$ Hz, *C*H$_{Cy}$), 27.4 (d, $^1J_{PC} = 27.1$ Hz, *C*H$_2$P), 27.1–26.9 (m, 3 *C*H$_{2\ Cy}$), 26.8 (d, $J_{PC} = 1.4$ Hz, *C*H$_{2\ Cy}$), 26.0 (br s, *C*H$_{2\ Cy}$), 19.6 (NCH$_2$CH$_2$*C*H$_2$), 13.6 (*C*H$_3$). $^{31}$P{$^1$H} NMR (161.98 MHz, CDCl$_3$): $\delta$ 28.7 (br s).

**Synthesis of 3-butyl-1-(3-((di-*tert*-butylphosphino)methyl)-phenyl)-1*H*-imidazol-3-ium bromide (L$^{tBu}$·HBr).** To a solution of **L$^{tBu}$**·2HBr (1.32 g, 2.54 mmol) in degassed methanol (15 mL) was added under argon a solution of NEt$_3$ (2 mL, 1.5 g, 15 mmol) in methanol (5 mL). After the resulting solution was stirred at r.t. for 1 h, all the volatiles were evaporated under reduced pressure. The oily residue was redissolved in CH$_2$Cl$_2$ and the solution was extracted three times with degassed water to remove the triethylammonium salt. The organic phase was dried over anhydrous MgSO$_4$ and concentrated under reduced pressure. Addition of a mixture of Et$_2$O and pentane precipitated **L$^{tBu}$**·HBr as a white powder that was isolated by filtration and dried under vacuum. Yield: 0.72 g (1.64 mmol), 65%. Anal. Calcd for C$_{22}$H$_{36}$BrN$_2$P (439.41): C, 60.13; H, 8.26; N, 6.38. Found: C, 59.90; H, 8.23; N, 6.87. $^1$H NMR (500.13 MHz, CD$_2$Cl$_2$): $\delta$ 11.17 (t, $^4J_{HH} = 1.6$ Hz, 1H, C*H*$_{imid.}$ H2), 7.71 (s, 1H, C*H*$_{arom.}$ H11), 7.66 (t, $^3J_{HH} = {}^4J_{HH} = 1.8$ Hz, 1H, C*H*$_{imid.}$ H4/H5), 7.64 (d, $^3J_{HH} = 8.2$ Hz, 1H, C*H*$_{arom.}$ H7/H9), 7.61 (t, $^3J_{HH} = {}^4J_{HH} = 1.7$ Hz, 1H, C*H*$_{imid.}$ H5/H4), 7.52 (d, $^3J_{HH} = 7.8$ Hz, 1H, C*H*$_{arom.}$ H9/H7), 7.46 (t, $^3J_{HH} = 7.8$ Hz, 1H, C*H*$_{arom.}$ H8), 4.57 (t, $^3J_{HH} = 7.2$ Hz, 2H, NC*H*$_2$), 2.94 (d, $^2J_{PH} = 2.6$ Hz, 2H, C*H*$_2$P), 1.97 (quint, $^3J_{HH} = 7.5$ Hz, 2H, NCH$_2$C*H*$_2$), 1.43 (sext, $^3J_{HH} = 7.5$ Hz, 2H, NCH$_2$CH$_2$C*H*$_2$), 1.13 (d, $^3J_{PH} = 11.0$ Hz, 18H, C(C*H*$_3$)$_3$), 0.98 (t, $^3J_{HH} = 7.4$ Hz, 3H, C*H*$_3$). $^{13}$C{$^1$H} NMR (125.77 MHz, CD$_2$Cl$_2$): $\delta$ 146.0 (d, $^2J_{PC} = 13.7$ Hz, *C*$_{arom.}$ C10), 136.6 (*C*H$_{imid.}$ C2), 134.8 (*C*$_{arom.}$ C6), 131.8 (d, $J_{PC} = 8.7$ Hz, *C*H$_{arom.}$), 130.5 (*C*H$_{arom.}$), 123.0 (*C*H$_{arom.}$), 122.7 (d, $J_{PC} = 9.7$ Hz, *C*H$_{arom.}$), 120.8 (*C*H$_{arom.}$), 119.2 (*C*H$_{arom.}$), 50.4 (N*C*H$_2$), 32.6 (NCH$_2$*C*H$_2$), 32.2 (d, $^1J_{PC} = 22.2$ Hz, *C*(CH$_3$)$_3$), 29.9 (d, $^2J_{PC} = 13.3$ Hz, C(*C*H$_3$)$_3$), 28.7 (d, $^1J_{PC} = 25.2$ Hz, *C*H$_2$P), 19.8 (NCH$_2$CH$_2$*C*H$_2$), 13.7 (*C*H$_3$). $^{31}$P{$^1$H} NMR (161.98 MHz, CD$_2$Cl$_2$): $\delta$ 32.0.

**Synthesis of 3-butyl-1-(3-((di-*tert*-butylphosphino)methyl)-phenyl)-1*H*-imidazol-3-ium tetrafluoroborate (L$^{tBu}$·HBF$_4$) by anion metathesis.** A solution of **L$^{tBu}$**·HBr (0.55 g, 1.25 mmol) and NaBF$_4$ (2.75 g, 25 mmol) in degassed ethanol was stirred overnight and evaporated to dryness. The oily residue was redissolved in CH$_2$Cl$_2$ and the solution was extracted three times with degassed water. The organic phase was dried over anhydrous MgSO$_4$ and concentrated under reduced pressure to afford a low melting point solid that was directly used in the next step. Yield: 0.40 g (0.90 mmol), 73%. $^1$H NMR (400.13 MHz, CD$_2$Cl$_2$): $\delta$ 9.18 (s, 1H, C*H*$_{imid.}$ H2), 7.63–7.55 (m, 3H, C*H*$_{imid.}$ H4/H5 + C*H*$_{arom.}$ H7/H9 + C*H*$_{arom.}$ H11), 7.49 (t, $^3J_{HH} = 7.8$ Hz, 1H, C*H*$_{arom.}$ H8), 7.47 (t, $^3J_{HH} = {}^4J_{HH} = 1.8$ Hz, 1H, C*H*$_{imid.}$ H5/H4), 7.40 (d, $^3J_{HH} = 7.8$ Hz, 1H, C*H*$_{arom.}$ H9/H7), 4.37 (t, $^3J_{HH} = 7.5$ Hz, 2H, NC*H*$_2$), 2.95 (d, $^2J_{PH} = 2.7$ Hz, 2H, C*H*$_2$P), 1.95 (quint, $^3J_{HH} = 7.5$ Hz, 2H, NCH$_2$C*H*$_2$), 1.45 (sext, $^3J_{HH} = 7.5$ Hz, 2H, NCH$_2$CH$_2$C*H*$_2$), 1.15 (d, $^3J_{PH} = 11.0$ Hz, 18H, C(C*H*$_3$)$_3$), 1.01 (t, $^3J_{HH} = 7.3$ Hz, 3H, C*H*$_3$). $^{31}$P{$^1$H} NMR (161.98 MHz, CD$_2$Cl$_2$): $\delta$ 37.4. $^{11}$B NMR (128.38 MHz, CD$_2$Cl$_2$): $\delta$ −1.0 (quint, $^1J_{BF} = 1.3$ Hz).

**Synthesis of 3-butyl-1-(3-((diphenylphosphino)methyl)-phenyl)-1*H*-imidazol-3-ium bromide (L$^{Ph}$·HBr).** To a solution of diphenylphosphine (0.59 g, 3.17 mmol) in THF (10 mL) cooled at −78 °C was added dropwise a solution of *n*BuLi in hexane (1.9 mL of a 1.6 M hexane solution, 3.04 mmol). The resulting orange solution was stirred at −78 °C for 45 min and added *via* cannula to a suspension of **A** (1.03 g, 2.76 mmol) (see Scheme 1) in THF (5 mL). The resulting mixture was allowed to reach r.t. and was stirred for 3 h. After removing all the volatiles under reduced pressure, the remaining orange oil was redissolved in CH$_2$Cl$_2$ and the solution was extracted three times with degassed water. The organic phase was dried over anhydrous MgSO$_4$ and evaporated to dryness under reduced pressure leading to a sticky powder. Stirring overnight with pentane afforded **L$^{Ph}$**·HBr as an off-white powder, which was isolated by filtration and dried under vacuum. Yield: 0.97 g (2.02 mmol), 73%. Single crystals suitable for X-ray diffraction were obtained by slow diffusion of pentane in a CH$_2$Cl$_2$ solution of **L$^{Ph}$**·HBr. Anal. Calcd for C$_{26}$H$_{28}$BrN$_2$P (479.40): C, 65.14; H, 5.89; N, 5.84. Found: C, 65.33; H, 5.92; N, 6.00. $^1$H NMR (400.13 MHz, CD$_2$Cl$_2$): $\delta$ 11.28 (t, $^4J_{HH} = 1.6$ Hz, 1H, C*H*$_{imid.}$ H2), 7.66 (br d, $^3J_{HH} = 8.0$ Hz, 1H, C*H*$_{arom.}$ H7/H9), 7.46–7.32 (m, 13H, 2 C*H*$_{imid.}$ + C*H*$_{arom.}$ H8 + 10 C*H*$_{PPh}$), 7.29 (q, $^4J_{HH} = {}^4J_{PH} = 1.8$ Hz, 1H, C*H*$_{arom.}$ H11), 7.21 (d, $^3J_{HH} = 7.6$ Hz, 1H, C*H*$_{arom.}$ H9/H7), 4.54 (t, $^3J_{HH} = 7.4$ Hz, 2H, NC*H*$_2$), 3.54 (s, 2H, C*H*$_2$P), 1.96 (quint, $^3J_{HH} = 7.5$ Hz, 2H, NCH$_2$C*H*$_2$), 1.43 (sext, $^3J_{HH} = 7.5$ Hz, 2H, NCH$_2$CH$_2$C*H*$_2$), 1.00 (t, $^3J_{HH} = 7.4$ Hz, 3H, C*H*$_3$). $^{13}$C{$^1$H} NMR (125.77 MHz, CD$_2$Cl$_2$): $\delta$ 141.1 (d, $^2J_{PC} = 8.0$ Hz, *C*$_{arom.}$ C10), 137.8 (d, $^1J_{PC} = 15.2$ Hz, *C*$_{PPh}$), 136.6 (*C*H$_{imid.}$ C2), 134.7 (d, $^4J_{PC} = 1.8$ Hz, *C*$_{arom.}$ C6), 133.3 (d, $J_{PC} = 18.8$ Hz, *C*H$_{PPh}$), 131.3 (d, $^3J_{PC} = 6.2$ Hz, *C*H$_{arom.}$ C9), 130.6 (d, $^4J_{PC} = 1.6$ Hz, *C*H$_{arom.}$ C8), 129.3 (*C*H$_{PPh}$), 128.9 (d, $J_{PC} = 6.6$ Hz, *C*H$_{PPh}$), 122.9 (*C*H$_{imid.}$ C4), 122.5 (d, $^3J_{PC} = 6.1$ Hz, *C*H$_{arom.}$ C11), 120.5 (*C*H$_{imid.}$ C5), 119.7 (d, $^5J_{PC} = 2.6$ Hz, *C*H$_{arom.}$ C7), 50.4 (N*C*H$_2$), 35.8 (d, $^1J_{PC} = 17.1$ Hz, *C*H$_2$P), 32.5 (NCH$_2$*C*H$_2$), 19.8 (NCH$_2$CH$_2$*C*H$_2$), 13.6 (*C*H$_3$). $^{31}$P{$^1$H} NMR (161.98 MHz, CD$_2$Cl$_2$): $\delta$ −8.5.

**Synthesis of 3-butyl-1-(3-((diphenylphosphonio)methyl)-phenyl)-1*H*-imidazol-3-ium (L$^{Ph}$·2HBr).** To a solution of **L$^{Ph}$**·HBr (0.35 g, 0.73 mmol) in CH$_2$Cl$_2$ (10 mL) was added methanol (0.1 mL, 79 mg, 2.5 mmol) and, dropwise, bromotrimethylsilane (0.11 mL, 128 mg, 0.84 mmol). After 2 h of stirring at room temperature, the solution was concentrated to *ca.* 2 mL under reduced pressure. Addition of Et$_2$O precipitated **L$^{Ph}$**·2HBr as an off-white powder that was collected by filtration and dried under vacuum. Yield: 0.40 g (0.72 mmol), 98%. $^1$H NMR (500.13 MHz, CDCl$_3$): $\delta$ 11.19 (t, $^4J_{HH} = 1.7$ Hz, 1H,

Open Access Article. Published on 11 February 2016. Downloaded on 10/20/2025 7:02:02 PM.
This article is licensed under a Creative Commons Attribution 3.0 Unported Licence.

C*H*$_{imid.}$ H2), 10.89 (br d, $^1J_{PH} \approx 500$ Hz, 1H, P*H*), 8.75 (t, $^3J_{HH} = {}^4J_{HH} = 1.8$ Hz, 1H, C*H*$_{imid.}$ H5), 8.63 (br s, 1H, C*H*$_{arom.}$ H11), 8.27 (dd, $J_{PH} = 14.0$ Hz, $^3J_{HH} = 7.5$ Hz, 4H, C*H*$_{PPh}$), 7.76 (dt, $^3J_{HH} = 8.3$ Hz, $^4J_{HH} = 2.1$ Hz, 1H, C*H*$_{arom.}$ H7), 7.67–7.61 (m, 3H, C*H*$_{arom.}$ H9 + 2 C*H*$_{PPh}$), 7.54 (dt, $^3J_{HH} = 7.7$ Hz, $J_{PH} = 3.2$ Hz, 4H, C*H*$_{PPh}$), 7.52 (overlapping t, $^3J_{HH} = {}^4J_{HH} = 1.7$ Hz, 1H, C*H*$_{imid.}$ H4), 6.90 (t, $^3J_{HH} = 7.8$ Hz, 1H, C*H*$_{arom.}$ H8), 5.01 (d, $^2J_{PH} = 16.1$ Hz, 2H, C*H*$_2$P), 4.41 (t, $^3J_{HH} = 7.4$ Hz, 2H, NC*H*$_2$), 1.97 (quint, $^3J_{HH} = 7.5$ Hz, 2H, NCH$_2$C*H*$_2$), 1.40 (sext, $^3J_{HH} = 7.5$ Hz, 2H, NCH$_2$CH$_2$C*H*$_2$), 0.96 (t, $^3J_{HH} = 7.4$ Hz, 3H, C*H*$_3$). $^{13}$C{$^1$H} NMR (125.77 MHz, CDCl$_3$): $\delta$ 135.5 (*C*H$_{imid.}$ C2), 135.0 (d, $^4J_{PC} = 2.6$ Hz, *C*H$_{PPh}$), 134.7 (d, $^4J_{PC} = 3.5$ Hz, *C*$_{arom.}$ C6), 134.0 (d, $J_{PC} = 10.7$ Hz, *C*H$_{PPh}$), 132.3 (d, $^3J_{PC} = 6.5$ Hz, *C*H$_{arom.}$ C9), 131.5 (d, $^2J_{PC} = 6.4$ Hz, *C*$_{arom.}$ C10), 131.0 (d, $^4J_{PC} = 2.6$ Hz, *C*H$_{arom.}$ C8), 130.3 (d, $J_{PC} = 13.0$ Hz, *C*H$_{PPh}$), 123.5 (d, $^3J_{PC} = 5.6$ Hz, *C*H$_{arom.}$ C11), 122.7 (*C*H$_{imid.}$ C4), 122.2 (*C*H$_{imid.}$ C5), 121.2 (d, $^5J_{PC} = 3.6$ Hz, *C*H$_{arom.}$ C7), 116.3 (d, $^1J_{PC} \approx 80$ Hz, *C*$_{PPh}$), 50.3 (N*C*H$_2$), 32.2 (NCH$_2$*C*H$_2$), 28.0 (d, $^1J_{PC} = 44.0$ Hz, *C*H$_2$P), 19.6 (NCH$_2$CH$_2$*C*H$_2$), 13.6 (*C*H$_3$). $^{31}$P NMR (161.98 MHz, CDCl$_3$): $\delta$ 0.1 (br d, $^1J_{PH} \approx 490$ Hz, *P*H).

**Synthesis of 3-butyl-1-(3-((diphenylphosphino)methyl)-phenyl)-1*H*-imidazol-3-ium tetrafluoroborate (L$^{Ph}$·HBF$_4$) by anion metathesis.** A solution of **L$^{Ph}$**·HBr (1.60 g, 3.34 mmol) and NaBF$_4$ (7.33 g, 66.8 mmol) in degassed ethanol was stirred overnight and evaporated to dryness. The oily residue was redissolved in CH$_2$Cl$_2$ and the solution was extracted three times with degassed water. The organic phase was dried over anhydrous MgSO$_4$ and concentrated under reduced pressure, leading to a cream-coloured oil. Stirring overnight with Et$_2$O afforded **L$^{Ph}$**·HBF$_4$ as an off-white powder, which was isolated by filtration and dried under vacuum. Yield: 1.49 g (3.06 mmol), 92%. $^1$H NMR (500.13 MHz, CDCl$_3$): $\delta$ 9.05 (t, $^4J_{HH} = 1.7$ Hz, 1H, C*H*$_{imid.}$ H2), 7.46–7.32 (m, 14H, 2 C*H*$_{imid.}$ + 2 C*H*$_{arom.}$ + 10 C*H*$_{PPh}$), 7.27 (dm, $^3J_{HH} = 7.1$ Hz, 1H, C*H*$_{arom.}$ H7/H9), 7.11 (q, $^4J_{HH} = {}^4J_{PH} = 1.8$ Hz, 1H, C*H*$_{arom.}$ H11), 4.34 (t, $^3J_{HH} = 7.5$ Hz, 2H, NC*H*$_2$), 3.54 (s, 2H, C*H*$_2$P), 1.92 (quint, $^3J_{HH} = 7.5$ Hz, 2H, NCH$_2$C*H*$_2$), 1.43 (sext, $^3J_{HH} = 7.4$ Hz, 2H, NCH$_2$CH$_2$C*H*$_2$), 1.00 (t, $^3J_{HH} = 7.4$ Hz, 3H, C*H*$_3$). $^{31}$P{$^1$H} NMR (161.98 MHz, CDCl$_3$): $\delta$ −8.3.

### General procedure for the synthesis of free carbene L$^R$

To a suspension of **L$^R$**·HBr (resp. **L$^R$**·2HBr) in diethyl ether (10 mL), precooled at −78 °C, was added a solution of 1.1 equiv. (resp. 2.1 equiv.) of KN(SiMe$_3$)$_2$ in diethyl ether (10 mL). The resulting suspension was allowed to reach room temperature and stirred for 1 h, giving a suspension of KBr in a yellow solution. Removal of the volatiles under reduced pressure, extraction of the resulting oil with pentane (25 mL) filtration and evaporation of the solvent gave **L$^R$** as a dark coloured oil.

**Synthesis of 3-butyl-1-(3-((dicyclohexylphosphino)methyl)-phenyl)-imidazol-2-ylidene (L$^{Cy}$).** Following the general procedure, **L$^{Cy}$** was synthesised from **L$^{Cy}$**·HBr (0.20 g, 0.41 mmol) and KN(SiMe$_3$)$_2$ (0.088 g, 0.44 mmol). Yield: 0.15 g (0.37 mmol), 90%. The oil turned green over a period of 1 h even when stored under inert atmosphere, however spectroscopic data remained unchanged. $^1$H NMR (400.13 MHz, C$_6$D$_6$): $\delta$ 8.20 (s, 1H, C*H*$_{arom.}$ H11), 7.67 (d, $^3J_{HH} = 7.8$ Hz, 1H, C*H*$_{arom.}$ H7/H9), 7.22 (d, $^3J_{HH} = 7.6$ Hz, 1H, C*H*$_{arom.}$ H9/H7), 7.15 (t, $^3J_{HH} = 7.8$ Hz, 1H, C*H*$_{arom.}$ H8), 7.06 (d, $^3J_{HH} = 1.6$ Hz, 1H, C*H*$_{imid.}$ H4/H5), 6.44 (br s, 1H, C*H*$_{imid.}$ H5/H4), 3.87 (t, $^3J_{HH} = 7.2$ Hz, 2H, NC*H*$_2$), 2.74 (s, 2H, C*H*$_2$P), 1.84–1.75 (m, 2H, C*H*$_{Cy}$), 1.74–1.47 (m, 10H, C*H*$_{2\ Cy}$), 1.60 (quint, $^3J_{HH} = 7.4$ Hz, 2H, NCH$_2$C*H*$_2$), 1.28–1.04 (m, 10H, C*H*$_{2\ Cy}$), 1.18 (sext, $^3J_{HH} = 7.4$ Hz, 2H, NCH$_2$CH$_2$C*H*$_2$), 0.78 (t, $^3J_{HH} = 7.3$ Hz, 3H, C*H*$_3$). $^{13}$C{$^1$H} NMR (100.62 MHz, C$_6$D$_6$): $\delta$ 216.2 (*C*$_{NHC}$), 143.1, 142.2 (d, $J_{PC} = 9.0$ Hz), 129.2, 127.1 (d, $J_{PC} = 7.6$ Hz), 122.3 (d, $J_{PC} = 7.4$ Hz), 119.7, 118.0, 116.9, 51.2 (N*C*H$_2$), 34.0 (d, $^1J_{PC} = 16.6$ Hz, *C*H$_{Cy}$), 33.8 (NCH$_2$*C*H$_2$), 30.3 (d, $J_{PC} = 13.2$ Hz, *C*H$_{2\ Cy}$), 29.81 (d, $^1J_{PC} = 21.5$ Hz, *C*H$_2$P), 29.79 (d, $J_{PC} = 10.0$ Hz, *C*H$_{2\ Cy}$), 27.7 (d, $J_{PC} = 9.7$ Hz, *C*H$_{2\ Cy}$), 27.6 (d, $J_{PC} = 7.6$ Hz, *C*H$_{2\ Cy}$), 26.9 (*C*H$_{2\ Cy}$), 20.0 (NCH$_2$CH$_2$*C*H$_2$), 13.9 (*C*H$_3$). $^{31}$P{$^1$H} NMR (161.98 MHz, C$_6$D$_6$): $\delta$ 0.0.

**Synthesis of 3-butyl-1-(3-((di-*tert*-butylphosphino)methyl)-phenyl)-imidazol-2-ylidene (L$^{tBu}$).** Following the general procedure, **L$^{tBu}$** was synthesised from **L$^{tBu}$**·2HBr (0.53 g, 1.02 mmol) and KN(SiMe$_3$)$_2$ (0.42 g, 2.12 mmol). Yield: 0.29 g (0.81 mmol), 79% (dark brown oil). $^1$H NMR (400.13 MHz, toluene-$d_8$): $\delta$ 8.09 (q, $^4J_{HH} = {}^4J_{PH} = 1.7$ Hz, 1H, C*H*$_{arom.}$ H11), 7.58 (d, $^3J_{HH} = 7.9$ Hz, 1H, C*H*$_{arom.}$ H7/H9), 7.23 (d, $^3J_{HH} = 7.8$ Hz, 1H, C*H*$_{arom.}$ H9/H7), 7.11 (t, $^3J_{HH} = 7.8$ Hz, 1H, C*H*$_{arom.}$ H8), 7.09 (d, $^3J_{HH} = 1.7$ Hz, 1H, C*H*$_{imid.}$ H4/H5), 6.52 (d, $^3J_{HH} = 1.6$ Hz, 1H, C*H*$_{imid.}$ H5/H4), 3.85 (t, $^3J_{HH} = 7.3$ Hz, 2H, NC*H*$_2$), 2.71 (d, $^2J_{PH} = 2.3$ Hz, 2H, C*H*$_2$P), 1.60 (quint, $^3J_{HH} = 7.4$ Hz, 2H, NCH$_2$C*H*$_2$), 1.19 (sext, $^3J_{HH} = 7.5$ Hz, 2H, NCH$_2$CH$_2$C*H*$_2$), 1.02 (d, $^3J_{PH} = 10.7$ Hz, 18H, C(C*H*$_3$)$_3$), 0.79 (t, $^3J_{HH} = 7.4$ Hz, 3H, C*H*$_3$). $^{13}$C{$^1$H} NMR (100.62 MHz, toluene-$d_8$): $\delta$ 215.9 (*C*$_{NHC}$), 143.3 (d, $J_{PC} = 13.0$ Hz), 142.9, 129.0, 127.3 (d, $J_{PC} = 9.7$ Hz), 122.3 (d, $J_{PC} = 8.6$ Hz), 119.7, 117.9, 116.9, 51.2 (N*C*H$_2$), 34.0 (NCH$_2$*C*H$_2$), 31.9 (d, $^1J_{PC} = 24.3$ Hz, *C*(CH$_3$)$_3$), 30.0 (d, $^2J_{PC} = 13.6$ Hz, C(*C*H$_3$)$_3$), 29.1 (d, $^1J_{PC} = 25.8$ Hz, *C*H$_2$P), 20.2 (NCH$_2$CH$_2$*C*H$_2$), 13.9 (*C*H$_3$). $^{31}$P{$^1$H} NMR (161.98 MHz, toluene-$d_8$): $\delta$ 33.1.

**Synthesis of 3-butyl-1-(3-((diphenylphosphino)methyl)-phenyl)-imidazol-2-ylidene (L$^{Ph}$).** Following the general procedure, **L$^{Ph}$** was synthesised from **L$^{Ph}$**·HBr (0.057 g, 0.12 mmol) and KN(SiMe$_3$)$_2$ (0.026 g, 0.13 mmol). Yield: 0.040 g (0.10 mmol), 84% (dark-green oil). $^1$H NMR (300.17 MHz, C$_6$D$_6$): $\delta$ 7.78 (dm, $^3J_{HH} = 7.9$ Hz, 1H, C*H*$_{arom.}$ H7/H9), 7.72 (q, $^4J_{HH} = {}^4J_{PH} = 1.7$ Hz, 1H, C*H*$_{arom.}$ H11), 7.39–7.30 (m, 4H, C*H*$_{PPh}$), 7.07–7.01 (m, 6H, C*H*$_{PPh}$), 7.01 (t, $^3J_{HH} = 7.8$ Hz, 1H, C*H*$_{arom.}$ H8), 6.89 (d, $^3J_{HH} = 1.7$ Hz, 1H, C*H*$_{imid.}$ H4/H5), 6.85 (dm, $^3J_{HH} = 7.8$ Hz, 1H, C*H*$_{arom.}$ H9/H7), 6.44 (d, $^3J_{HH} = 1.7$ Hz, 1H, C*H*$_{imid.}$ H5/H4), 3.86 (t, $^3J_{HH} = 7.2$ Hz, 2H, NC*H*$_2$), 3.24 (s, 2H, C*H*$_2$P), 1.60 (quint, $^3J_{HH} = 7.3$ Hz, 2H, NCH$_2$C*H*$_2$), 1.18 (sext, $^3J_{HH} = 7.4$ Hz, 2H, NCH$_2$CH$_2$C*H*$_2$), 0.79 (t, $^3J_{HH} = 7.4$ Hz, 3H, C*H*$_3$). $^{13}$C{$^1$H} NMR (75.49 MHz, C$_6$D$_6$): $\delta$ 216.1 (*C*$_{NHC}$), 142.9, 139.09 (d, $J_{PC} = 16.5$ Hz, *C*$_{PPh}$), 139.05 (d, $J_{PC} = 8.2$ Hz), 133.4 (d, $J_{PC} = 18.6$ Hz, *C*H$_{PPh}$), 129.2 (d, $J_{PC} = 1.6$ Hz), 128.8 (*C*H$_{PPh}$), 128.6 (d, $J_{PC} = 6.4$ Hz, *C*H$_{PPh}$), 127.0 (d, $J_{PC} = 6.8$ Hz), 122.0 (d, $J_{PC} = 6.7$ Hz), 119.7, 118.8 (d, $J_{PC} = 2.7$ Hz), 116.9, 51.2 (N*C*H$_2$), 36.3 (d, $^1J_{PC} = 16.8$ Hz, *C*H$_2$P), 33.8 (NCH$_2$*C*H$_2$), 20.0 (NCH$_2$CH$_2$*C*H$_2$), 13.9 (*C*H$_3$). $^{31}$P{$^1$H} NMR (161.98 MHz, C$_6$D$_6$): $\delta$ −9.9.

 This journal is © The Royal Society of Chemistry 2016

Open Access Article. Published on 11 February 2016. Downloaded on 10/20/2025 7:02:02 PM.
This article is licensed under a Creative Commons Attribution 3.0 Unported Licence.

**Synthesis of the tetranuclear silver cluster $[Ag_2(\mu_3\text{-}Br)_2(\mu\text{-}PPh_2\text{-}NHC,\kappa P,\kappa C^{NHC})]_2$ ($[Ag_4Br_4(L^{Ph})_2]$) (route (b)).** $L^{Ph}\cdot$2HBr (0.40 g, 0.72 mmol) and $Ag_2O$ (0.185 g, 0.80 mmol) were charged in a Schlenk flask along with molecular sieves 4 Å. Degassed acetonitrile (20 mL) was added and the mixture was stirred for 2 days at 40 °C under exclusion of light. After evaporation of the solvent under reduced pressure, the remaining slurry was extracted twice with $CH_2Cl_2$, and the resulting solution was filtered over Celite® and concentrated to *ca.* 1 mL. Complex $[Ag_4Br_4(L^{Ph})_2]$ was precipitated by addition of $Et_2O$. The white powder was collected by filtration and dried under vacuum. Yield: 0.46 g (0.30 mmol), 83% based on the ligand. Single crystals suitable for X-ray diffraction were obtained by slow diffusion of $Et_2O$ in a $CH_2Cl_2$ solution of the complex. Anal. Calcd for $C_{52}H_{54}Ag_4Br_4N_4P_2$ (1548.05): C, 40.34; H, 3.52; N, 3.62. Found: C, 40.23; H, 3.61; N, 3.45. $^1$H NMR (500.13 MHz, $CD_2Cl_2$): $\delta$ 8.55 (q, $^4J_{HH}$ = $^4J_{PH}$ = 1.8 Hz, 1H, C*H*$_{arom.}$ H11), 7.79–7.74 (m, 4H, C*H*$_{PPh}$), 7.48–7.38 (m, 6H, C*H*$_{PPh}$), 7.24 (d, $^3J_{HH}$ = 1.7 Hz, 1H, C*H*$_{imid.}$ H4/H5), 7.18 (dm, $^3J_{HH}$ = 7.8 Hz, 1H, C*H*$_{arom.}$ H7), 7.08 (d, $^3J_{HH}$ = 1.7 Hz, 1H, C*H*$_{imid.}$ H5/H4), 7.07 (t, $^3J_{HH}$ = 7.8 Hz, 1H, C*H*$_{arom.}$ H8), 6.34 (br d, $^3J_{HH}$ = 7.7 Hz, 1H, C*H*$_{arom.}$ H9), 4.27 (t, $^3J_{HH}$ = 7.4 Hz, 2H, NC*H*$_2$), 3.69 (d, $^2J_{PH}$ = 7.8 Hz, 2H, C*H*$_2$P), 1.84 (quint, $^3J_{HH}$ = 7.5 Hz, 2H, NCH$_2$C*H*$_2$), 1.41 (sext, $^3J_{HH}$ = 7.5 Hz, 2H, NCH$_2$CH$_2$C*H*$_2$), 0.94 (t, $^3J_{HH}$ = 7.5 Hz, 3H, C*H*$_3$). $^{13}$C{$^1$H} NMR (125.77 MHz, $CD_2Cl_2$): $\delta$ 186.5 (br s, $\Delta\nu_{1/2}$ = 12 Hz, $C_{NHC}$), 141.4 (d, $J_{PC}$ = 3.3 Hz, $C_{arom.}$ C6/C10), 136.9 (d, $J_{PC}$ = 2.4 Hz, $C_{arom.}$ C10/C6), 134.0 (d, $J_{PC}$ = 16.3 Hz, *C*H$_{PPh}$), 132.8 (d, $^1J_{PC}$ = 21.1 Hz, $C_{PPh}$), 130.8 (d, $J_{PC}$ = 1.6 Hz, *C*H$_{PPh}$), 129.5 (d, $^3J_{PC}$ = 4.8 Hz, *C*H$_{arom.}$ C9), 129.0 (d, $J_{PC}$ = 9.6 Hz, *C*H$_{PPh}$), 128.8 (d, $^4J_{PC}$ = 2.8 Hz, *C*H$_{arom.}$ C8), 126.8 (d, $^3J_{PC}$ = 5.2 Hz, *C*H$_{arom.}$ C11), 121.4 (d, $^5J_{PC}$ = 3.5 Hz, *C*H$_{arom.}$ C7), 121.2 (*C*H$_{imid.}$ C4/C5), 121.1 (*C*H$_{imid.}$ C5/C4), 52.3 (N*C*H$_2$), 35.5 (d, $^1J_{PC}$ = 8.8 Hz, *C*H$_2$P), 34.0 (NCH$_2$*C*H$_2$), 20.2 (NCH$_2$CH$_2$*C*H$_2$), 14.0 (*C*H$_3$). $^{31}$P{$^1$H} NMR (161.98 MHz, $CD_2Cl_2$): $\delta$ 3.0 (br s). MS (ESI+): *m*/*z* (%) 1540.68 (<1) $[M + H]^+$, 1248.96 (100) $[M - 2Ag - Br + 2H]^+$ *i.e.* $[C_{52}H_{56}Ag_2Br_3N_4P_2]^+$ with the corresponding isotopic pattern.

### General procedure for the synthesis of silver(I) complexes $[Ag_2(L^R)_2](BF_4)_2$

$L^R\cdot HBF_4$ and $Ag_2O$ (0.55 equiv.) were charged in a Schlenk flask along with molecular sieves 4 Å. Degassed acetonitrile (15 mL) was added and the mixture was stirred for 2 days at 40 °C under exclusion of light. After evaporation of the solvent under reduced pressure, the remaining slurry was extracted twice with $CH_2Cl_2$ and the resulting solution was filtered over Celite® and concentrated to *ca.* 1 mL. The complex $[Ag_2(L^R)_2](BF_4)_2$ was precipitated with diethyl ether. The white powder was collected by filtration and dried under vacuum.

**Synthesis of $[Ag(\mu\text{-}PPh_2\text{-}NHC,\kappa P,\kappa C^{NHC})]_2(BF_4)_2$ ($[Ag_2(L^{Ph})_2](BF_4)_2$).** Following the general procedure, $[Ag_2(L^{Ph})_2](BF_4)_2$ was synthesised from $L^{Ph}\cdot HBF_4$ (0.12 g, 0.25 mmol) and $Ag_2O$ (0.032 g, 0.14 mmol). Yield: 0.13 g (0.11 mmol), 85% based on the ligand. Single crystals suitable for X-ray diffraction were obtained by slow diffusion of $Et_2O$ in a $CH_2Cl_2$ or $CH_3CN$ solution of the complex. Anal. Calcd for $C_{52}H_{54}Ag_2B_2F_8N_4P_2\cdot 0.6CH_2Cl_2$ (1237.28): C, 51.06; H, 4.50; N, 4.53. Found: C, 50.98; H, 4.42; N, 4.72. Examination of the $^1$H and $^{31}$P{$^1$H} NMR spectra revealed the presence of the "head-to-tail" and "head-to-head" isomers in a *ca.* 4 : 1 HT/HH ratio in $CD_2Cl_2$ (see text) and 1 : 1.1 in $CD_3CN$. $^1$H NMR (400.13 MHz, $CD_2Cl_2$): $\delta$ 8.00 (br q, $^4J_{HH}$ = $^4J_{PH}$ = 1.6 Hz, 0.8H, C*H*$_{arom.}$ H11), 7.64 (t, $^3J_{HH}$ = $^4J_{HAg}$ = 1.7 Hz, 0.8H, C*H*$_{imid.}$), 7.63–7.22 (m, 11.6H, C*H*$_{arom.}$), 7.17 (t, $^3J_{HH}$ = $^4J_{HAg}$ = 1.7 Hz, 0.8H, C*H*$_{imid.}$), 7.09 (t, $^3J_{HH}$ = 7.9 Hz, 0.2H, C*H*$_{arom.}$ H8), 7.04 (t, $^3J_{HH}$ = 7.8 Hz, 0.8H, C*H*$_{arom.}$ H8), 6.92 (s, 0.2H, C*H*$_{arom.}$), 6.60 (d, $^3J_{HH}$ = 7.7 Hz, C*H*$_{arom.}$ H7/H9), 4.30 (t, $^3J_{HH}$ = 7.3 Hz, 1.6H, NC*H*$_2$), 4.20 (t, $^3J_{HH}$ = 7.3 Hz, 0.4H, NC*H*$_2$), 3.93 (AB part of an ABX spin system with A = B = H and X = P, *J* = 10.5, 4.6 Hz, 1.6H, C*H*$_2$P), 3.89–3.82 (br s, 0.4H, C*H*$_2$P), 1.91 (quint, $^3J_{HH}$ = 7.4 Hz, 0.4H, NCH$_2$C*H*$_2$), 1.82 (quint, $^3J_{HH}$ = 7.4 Hz, 1.6H, NCH$_2$C*H*$_2$), 1.40 (sext, $^3J_{HH}$ = 7.4 Hz, 2H, NCH$_2$CH$_2$C*H*$_2$), 1.03 (t, $^3J_{HH}$ = 7.3 Hz, 0.6H, C*H*$_3$), 0.96 (t, $^3J_{HH}$ = 7.4 Hz, 2.4H, C*H*$_3$). $^{13}$C{$^1$H} NMR (125.77 MHz, $CD_2Cl_2$): $\delta$ $C_{NHC}$ peak not observed, 140.7 ($C_{arom.}$), 137.6 ($C_{arom.}$), 133.6 (dd, $J_{PC}$ = 14.6 Hz, $J_{AgC}$ = 2.3 Hz, *C*H$_{PPh}$), 132.1 (d, $J_{PC}$ = 1.8 Hz, *C*H$_{PPh}$), 130.4 (d, *J* = 5.4 Hz, *C*H$_{arom.}$), 129.9 (d, *J* = 2.9 Hz, *C*H$_{arom.}$), 129.8 (d, $J_{PC}$ = 10.4 Hz, *C*H$_{PPh}$), 129.1 (dd, $^1J_{PC}$ = 36.7 Hz, $^2J_{AgC}$ = 4.4 Hz, $C_{PPh}$), 126.3 (d, *J* = 8.4 Hz, *C*H$_{arom.}$), 122.8 (d, *J* = 5.5 Hz, *C*H$_{arom.}$), 122.7 (d, *J* = 4.0 Hz, *C*H$_{arom.}$), 122.2 (d, *J* = 6.3 Hz, *C*H$_{arom.}$), 52.3 (N*C*H$_2$), 34.4 (d, $^1J_{PC}$ = 17.1 Hz, *C*H$_2$P), 33.9 (NCH$_2$*C*H$_2$), 19.9 (NCH$_2$CH$_2$*C*H$_2$), 13.9 (*C*H$_3$). $^{31}$P{$^1$H} NMR (161.98 MHz, $CD_2Cl_2$): $\delta$ 25.2 (two doublets, $^1J_{P-107Ag}$ = 503 Hz, $^1J_{P-109Ag}$ = 581 Hz, integrating for 0.8P), 17.6 (two doublets, $^1J_{P-107Ag}$ ≈ 515 Hz, $^1J_{P-109Ag}$ ≈ 595 Hz, integrating for 0.2P). $^{11}$B NMR (128.38 MHz, $CD_2Cl_2$): $\delta$ −0.9 (quint, $^1J_{BF}$ = 1.5 Hz).

$^1$H NMR (400.13 MHz, $CD_3CN$): $\delta$ 7.67–7.25 (m, 13.6H, C*H*$_{arom.}$), 7.14–6.88 (br s, 2H, C*H*$_{arom.}$), 6.82–6.60 (br s, 0.4H, C*H*$_{arom.}$), 5.45 (s, 0.4H, residual $CH_2Cl_2$), 4.20 (t, $^3J_{HH}$ = 7.3 Hz, 2H, NC*H*$_2$), 3.70 (br s, 2H, C*H*$_2$P), 1.91–1.69 (br s, 2H, NCH$_2$C*H*$_2$), 1.37 (sext, $^3J_{HH}$ = 7.4 Hz, 2H, NCH$_2$CH$_2$C*H*$_2$), 0.98 (t, $^3J_{HH}$ = 7.3 Hz, 3H, C*H*$_3$). $^{31}$P{$^1$H} NMR (161.98 MHz, $CD_3CN$): $\delta$ 21.3 (two doublets, $^1J_{P-107Ag}$ ≈ 500 Hz, $^1J_{P-109Ag}$ ≈ 580 Hz, integrating for 1.0P), 11.2 (two doublets, $^1J_{P-107Ag}$ ≈ 475 Hz, $^1J_{P-109Ag}$ ≈ 550 Hz, integrating for 1.1P).

**Synthesis of $[Ag(\mu\text{-}PtBu_2\text{-}NHC,\kappa P,\kappa C^{NHC})]_2(BF_4)_2$ ($[Ag_2(L^{tBu})_2](BF_4)_2$).** Following the general procedure, $[Ag_2(L^{tBu})_2](BF_4)_2$ was synthesised from $L^{tBu}\cdot HBF_4$ (0.40 g, 0.90 mmol) and $Ag_2O$ (0.12 g, 0.50 mmol). Yield: 0.34 g (0.31 mmol), 68% based on the ligand. Single crystals suitable for X-ray diffraction were obtained by slow diffusion of toluene in a $CH_2Cl_2$ solution of the complex. Anal. Calcd for $C_{44}H_{70}Ag_2B_2F_8N_4P_2$ (1106.36): C, 47.77; H, 6.38; N, 5.06. Found: C, 47.88; H, 6.20; N, 5.02. Examination of the $^1$H and $^{31}$P{$^1$H} NMR spectra revealed the presence of the "head-to-head" and "head-to-tail" isomers in a HH/HT ratio of *ca.* 1 : 2 in $CD_2Cl_2$ (see text). $^1$H NMR (400.13 MHz, $CD_2Cl_2$): 7.74 (br s, 0.7H, C*H*$_{arom.}$ H11), 7.66 (t, $^3J_{HH}$ = $^4J_{HAg}$ = 1.7 Hz, 0.7H, C*H*$_{imid.}$), 7.58 (t, $^3J_{HH}$ = $^4J_{HAg}$ = 1.8 Hz, 0.3H, C*H*$_{imid.}$), 7.50 (br s, 0.3H, C*H*$_{arom.}$ H11), 7.40 (br d, $^3J_{HH}$ = 7.8 Hz, 0.3H, C*H*$_{arom.}$ H7/H9), 7.35 (br d, $^3J_{HH}$ = 7.9 Hz, 0.7H, C*H*$_{arom.}$ H7/H9), 7.31 (t, $^3J_{HH}$ = $^4J_{HAg}$ = 1.8 Hz, 0.3H, C*H*$_{imid.}$), 7.31–7.26 (overlapping m, 0.7H, C*H*$_{arom.}$ H9/H7), 7.28 (t, $^3J_{HH}$ = $^4J_{HAg}$ = 1.7 Hz, 0.7H, C*H*$_{imid.}$), 7.23–7.19 (overlapping m, 0.3H, C*H*$_{arom.}$ H9/H7), 7.23 (t, $^3J_{HH}$ = 7.8 Hz, 0.7H, C*H*$_{arom.}$ H8), 7.14

Open Access Article. Published on 11 February 2016. Downloaded on 10/20/2025 7:02:02 PM.
This article is licensed under a Creative Commons Attribution 3.0 Unported Licence.

(t, $^3J_{HH}$ = 7.8 Hz, 0.3H, C*H*$_{arom.}$ H8), 4.25 (t, $^3J_{HH}$ = 7.3 Hz, 0.6H, NC*H*$_2$), 4.18 (t, $^3J_{HH}$ = 7.3 Hz, 1.4H, NC*H*$_2$), 3.32 (AB part of an ABX spin system with A = B = H and X = P, *J* = 10.1 Hz, 4.2 Hz, 1.4H, C*H*$_2$P), 3.27 (AB part of an ABX spin system with A = B = H and X = P, *J* = 9.0 Hz, 3.7 Hz, 0.6H, C*H*$_2$P), 1.96 (quint, $^3J_{HH}$ = 7.5 Hz, 0.6H, NCH$_2$C*H*$_2$), 1.86 (quint, $^3J_{HH}$ = 7.5 Hz, 1.4H, NCH$_2$C*H*$_2$), 1.46 (sext, $^3J_{HH}$ = 7.5 Hz, 2H, NCH$_2$CH$_2$C*H*$_2$), 1.40 (virtual t, $|^3J_{PCH} + {}^5J_{PH}|$ = 14.9 Hz, 6H, C(C*H*$_3$)$_3$), 1.29 (d, $^3J_{PH}$ = 14.7 Hz, 12H, C(C*H*$_3$)$_3$), 1.04 (t, $^3J_{HH}$ = 7.3 Hz, 1H, C*H*$_3$), 1.01 (t, $^3J_{HH}$ = 7.4 Hz, 2H, C*H*$_3$). $^{13}$C{$^1$H} NMR (125.77 MHz, CD$_2$Cl$_2$): $\delta$ 178.8 (two doublets, $^1J_{C-107Ag}$ = 183 Hz, $^1J_{C-109Ag}$ = 212 Hz, minor $C_{NHC}$), 178.5 (two dd, $^1J_{C-107Ag}$ = 190 Hz, $^1J_{C-109Ag}$ = 219 Hz, $^2J_{P-Ag-C}$ = 62 Hz, major $C_{NHC}$), 141.3 (minor $C_{arom.}$), 141.1 (major $C_{arom.}$), 140.6 (minor $C_{arom.}$), 140.2 (major $C_{arom.}$), 131.1 (d, $J_{PC}$ = 5.7 Hz, major *C*H$_{arom.}$), 130.7 (minor *C*H$_{imid.}$), 130.3 (major *C*H$_{imid.}$), 129.1 (virtual t, $|^nJ_{PC} + {}^{n+2}J_{PAgPC}|$ = 8.2 Hz, minor *C*H$_{arom.}$), 125.9 (d, $J_{PC}$ = 9.6 Hz, major *C*H$_{arom.}$), 125.2 (virtual t, $|^nJ_{PC} + {}^{n+2}J_{PAgPC}|$ = 6.0 Hz, minor *C*H$_{arom.}$), 123.0 (d, $J_{PC}$ = 5.8 Hz, major *C*H$_{arom.}$), 122.9 (d, $J_{PC}$ = 5.8 Hz, minor *C*H$_{arom.}$), 122.8 (d, *J* = 5.2 Hz, minor *C*H$_{arom.}$), 122.5 (minor *C*H$_{imid.}$), 122.3 (major *C*H$_{imid.}$), 122.1 (d, *J* = 5.3 Hz, major *C*H$_{arom.}$), 52.7 (minor N*C*H$_2$), 52.6 (major N*C*H$_2$), 35.3 (doublet of virtual t, $|^1J_{PC} + {}^3J_{PAgPC}|$ = 11.9 Hz, $^2J_{CAg}$ = 3.9 Hz, minor *C*(CH$_3$)$_3$), 34.8 (dd, $^1J_{PC}$ = 12.2 Hz, $^2J_{CAg}$ = 3.7 Hz, major *C*(CH$_3$)$_3$), 34.3 (major NCH$_2$*C*H$_2$), 33.9 (minor NCH$_2$*C*H$_2$), 29.95–29.75 (m, C(*C*H$_3$)$_3$), 27.0 (d, $^1J_{PC}$ = 12.9 Hz, major *C*H$_2$P), 26.4 (virtual t, $|^1J_{PC} + {}^3J_{PAgPC}|$ = 14.0 Hz, minor *C*H$_2$P), 20.3 (minor NCH$_2$CH$_2$*C*H$_2$), 20.1 (major NCH$_2$CH$_2$*C*H$_2$), 13.84 (major CH$_3$), 13.81 (minor CH$_3$). $^{31}$P{$^1$H} NMR (161.98 MHz, CD$_2$Cl$_2$): $\delta$ 73.6 (two doublets, $^1J_{P-107Ag}$ = 460 Hz, $^1J_{P-109Ag}$ = 530 Hz, integrating for 1P), 72.4 (two doublets, $^1J_{P-107Ag}$ = 477 Hz, $^1J_{P-109Ag}$ = 552 Hz, integrating for 2P).

### General procedure for the synthesis of copper(I) complexes [Cu$_2$Br$_2$(L$^R$)$_2$]

To a suspension of **L$^R$**·HBr in THF (5 mL) was added a solution of mesityl copper(I) (1.0 equiv. based on Cu) in THF (5 mL) at room temperature. The resulting clear solution was stirred at room temperature for 24 h. After evaporation of the solvent under reduced pressure, the solid residue was washed with diethyl ether and redissolved in CH$_2$Cl$_2$. Addition of pentane precipitated [Cu$_2$Br$_2$(**L$^R$**)$_2$] as a white powder that was collected and dried under vacuum.

**Synthesis of [CuBr(μ-PCy$_2$-NHC,κ*P*,κ*C*$^{NHC}$)]$_2$ [Cu$_2$Br$_2$(L$^{Cy}$)$_2$].** Following the general procedure, [Cu$_2$Br$_2$(**L$^{Cy}$**)$_2$] was synthesised from **L$^{Cy}$**·HBr (0.19 g, 0.38 mmol) and mesityl copper (I) (0.073 g, 0.40 mmol). Yield: 0.20 g (0.18 mmol), 95% based on the ligand. Single crystals suitable for X-ray diffraction were obtained by slow vapour diffusion of Et$_2$O in a THF solution of the complex. Anal. Calcd for C$_{52}$H$_{78}$Br$_2$Cu$_2$N$_4$P$_2$ (1108.05): C, 56.37; H, 7.10; N, 5.06. Found: C, 56.52; H, 7.31; N, 4.92. $^1$H NMR (400.13 MHz, CD$_2$Cl$_2$): $\delta$ 7.77 (d, $^3J_{HH}$ = 7.5 Hz, 1H, C*H*$_{arom.}$ H7), 7.26 (t, $^3J_{HH}$ = 7.6 Hz, 1H, C*H*$_{arom.}$ H8), 7.17 (s, 1H, C*H*$_{arom.}$ H11), 7.09 (d, $^3J_{HH}$ = 7.5 Hz, 1H, C*H*$_{arom.}$ H9), 6.91 (s, 1H, C*H*$_{imid.}$ H4), 6.70 (s, 1H, C*H*$_{imid.}$ H5), 4.20 (t, $^3J_{HH}$ = 7.4 Hz, 2H, NC*H*$_2$), 2.78 (d, $^2J_{PH}$ = 6.5 Hz, 2H, C*H*$_2$P), 1.97–1.53 (m, 12H, Cy), 1.80 (quint, $^3J_{HH}$ = 7.6 Hz, 2H, NCH$_2$C*H*$_2$), 1.50–1.12 (m, 10H, Cy), 1.41 (sext, $^3J_{HH}$ = 7.5 Hz, 2H, NCH$_2$CH$_2$C*H*$_2$), 0.96 (t, $^3J_{HH}$ = 7.4 Hz, 3H, C*H*$_3$). $^{13}$C{$^1$H} NMR (125.77 MHz, CD$_2$Cl$_2$): $\delta$ 185.1 (d, $^2J_{PC}$ = 47.0 Hz, $C_{NHC}$), 140.7 ($C_{arom.}$ C6), 139.0 ($C_{arom.}$ C10), 129.6 (*C*H$_{arom.}$ C8), 129.4 (d, $^3J_{PC}$ = 3.1 Hz, *C*H$_{arom.}$ C9), 123.7 (d, $^3J_{PC}$ = 4.5 Hz, *C*H$_{arom.}$ C11), 122.5 (*C*H$_{arom.}$ C7), 120.9 (*C*H$_{imid.}$ C4), 119.3 (*C*H$_{imid.}$ C5), 51.4 (N*C*H$_2$), 34.3 (NCH$_2$*C*H$_2$), 34.0 (d, $^1J_{PC}$ = 14.6 Hz, *C*H$_{Cy}$), 29.5 (d, $^3J_{PC}$ = 2.5 Hz, *C*H$_{2\ Cy}$), 29.2 (d, $^3J_{PC}$ = 4.0 Hz, *C*H$_{2\ Cy}$), 28.9 (d, $^1J_{PC}$ = 8.6 Hz, *C*H$_2$P), 27.6 (d, $^2J_{PC}$ = 11.8 Hz, *C*H$_{2\ Cy}$), 27.3 (d, $^2J_{PC}$ = 10.2 Hz, *C*H$_{2\ Cy}$), 26.5 (*C*H$_{2\ Cy}$), 20.4 (NCH$_2$CH$_2$*C*H$_2$), 14.0 (*C*H$_3$). $^{31}$P{$^1$H} NMR (161.98 MHz, CD$_2$Cl$_2$): $\delta$ 7.4.

**Synthesis of [CuBr(μ-P*t*Bu$_2$-NHC,κ*P*,κ*C*$^{NHC}$)]$_2$ ([Cu$_2$Br$_2$(L$^{tBu}$)$_2$]).** Following the general procedure, [Cu$_2$Br$_2$(**L$^{tBu}$**)$_2$] was synthesised from **L$^{tBu}$**·HBr (0.18 g, 0.41 mmol) and mesityl copper (I) (0.078 g, 0.43 mmol). Yield: 0.18 g (0.17 mmol), 85% based on the ligand. Single crystals suitable for X-ray diffraction were obtained by slow diffusion of toluene in a CH$_2$Cl$_2$ solution of the complex. Anal. Calcd for C$_{44}$H$_{70}$Br$_2$Cu$_2$N$_4$P$_2$ (1003.90): C, 52.64; H, 7.03; N, 5.58. Found: C, 52.61; H, 7.22; N, 5.67. $^1$H NMR (400.13 MHz, CD$_2$Cl$_2$): $\delta$ 8.12 (d, $^3J_{HH}$ = 7.3 Hz, 1H, C*H*$_{arom.}$ H7), 7.44 (s, 1H, C*H*$_{arom.}$ H11), 7.17 (t, $^3J_{HH}$ = 7.6 Hz, 1H, C*H*$_{arom.}$ H8), 7.08 (d, $^3J_{HH}$ = 7.5 Hz, 1H, C*H*$_{arom.}$ H9), 6.93 (d, $^3J_{HH}$ = 1.4 Hz, 1H, C*H*$_{imid.}$ H4), 6.67 (s, 1H, C*H*$_{imid.}$ H5), 4.27 (br s, 2H, NC*H*$_2$), 2.98 (d, $^2J_{PH}$ = 7.4 Hz, 2H, C*H*$_2$P), 2.01 (quint, $^3J_{HH}$ = 7.6 Hz, 2H, NCH$_2$C*H*$_2$), 1.50 (sext, $^3J_{HH}$ = 7.4 Hz, 2H, NCH$_2$CH$_2$C*H*$_2$), 1.56–0.98 (br s, 18H, C(C*H*$_3$)$_3$), 1.01 (t, $^3J_{HH}$ = 7.3 Hz, 3H, C*H*$_3$). $^{13}$C{$^1$H} NMR (125.77 MHz, CD$_2$Cl$_2$): $\delta$ 185.2 (d, $^2J_{PC}$ = 46.0 Hz, $C_{NHC}$), 140.7 ($C_{arom.}$ C6), 140.3 ($C_{arom.}$ C10), 130.5 (d, $J_{PC}$ = 3.2 Hz, *C*H$_{arom.}$ C9), 129.6 (*C*H$_{arom.}$ C8), 123.5 (*C*H$_{arom.}$ C7), 122.8 (*C*H$_{arom.}$ C11), 121.2 (*C*H$_{imid.}$ C4), 119.3 (*C*H$_{imid.}$ C5), 51.5 (N*C*H$_2$), 34.7 (br d, $^1J_{PC}$ = 7.0 Hz, *C*(CH$_3$)$_3$), 34.1 (NCH$_2$*C*H$_2$), 29.8 (br s, C(*C*H$_3$)$_3$), 27.9 (d, $^1J_{PC}$ = 5.9 Hz, *C*H$_2$P), 20.5 (NCH$_2$CH$_2$*C*H$_2$), 14.0 (*C*H$_3$). $^{31}$P{$^1$H} NMR (161.98 MHz, CD$_2$Cl$_2$): $\delta$ 32.2.

**Synthesis of [CuBr(μ-PPh$_2$-NHC,κ*P*,κ*C*$^{NHC}$)]$_2$ ([Cu$_2$Br$_2$(L$^{Ph}$)$_2$]).** Following the general procedure, [Cu$_2$Br$_2$(**L$^{Ph}$**)$_2$] was synthesised from **L$^{Ph}$**·HBr (0.13 g, 0.27 mmol) and mesityl copper (I) (0.057 g, 0.31 mmol). Yield: 0.13 g (0.12 mmol), 90% based on the ligand. Anal. Calcd for C$_{52}$H$_{54}$Br$_2$Cu$_2$N$_4$P$_2$ (1083.86): C, 57.62; H, 5.02; N, 5.17. Found: C, 55.66; H, 4.86; N, 4.92. Better elemental analyses and single crystals suitable for X-ray diffraction studies could not be obtained despite several attempts. $^1$H NMR (300.13 MHz, CD$_2$Cl$_2$): $\delta$ 7.61 (m, 4H, C*H*$_{PPh}$), 7.50–7.30 (m, 8H, C*H*$_{imid.}$ + C*H*$_{arom.}$ + 6 C*H*$_{PPh}$), 7.03 (br s, 1H, C*H*$_{arom.}$), 6.96 (d, $^3J_{HH}$ = 1.6 Hz, 1H, C*H*$_{imid.}$), 6.72 (t, $^3J_{HH}$ = 7.5 Hz, 1H, C*H*$_{arom.}$), 6.44 (d, $^3J_{HH}$ = 7.3 Hz, 1H, C*H*$_{arom.}$), 4.13 (t, $^3J_{HH}$ = 7.4 Hz, 2H, NC*H*$_2$), 3.24 (br s, 2H, C*H*$_2$P), 1.65 (quint, $^3J_{HH}$ = 7.5 Hz, 2H, NCH$_2$C*H*$_2$), 1.24 (sext, $^3J_{HH}$ = 7.4 Hz, 2H, NCH$_2$CH$_2$C*H*$_2$), 0.85 (t, $^3J_{HH}$ = 7.3 Hz, C*H*$_3$). $^{13}$C{$^1$H} NMR (125.77 MHz, CD$_2$Cl$_2$): $\delta$ 183.7 (br s, $C_{NHC}$), 140.4 ($C_{arom.}$), 137.1 ($C_{arom.}$), 133.7 (d, $J_{PC}$ = 13.8 Hz, *C*H$_{PPh}$), 133.4 (d, $^1J_{PC}$ = 25.4 Hz, $C_{PPh}$), 130.4 (*C*H$_{PPh}$), 129.4 (*C*H$_{arom.}$), 129.1 (br s, *C*H$_{arom.}$), 128.9 (d, $J_{PC}$ = 8.5 Hz, *C*H$_{PPh}$), 124.1 (br s, *C*H$_{arom.}$), 121.2 (*C*H$_{arom.}$), 120.9 (*C*H$_{arom.}$), 119.4 (br s, *C*H$_{arom.}$), 51.5 (N*C*H$_2$), 34.7 (d, $^1J_{PC}$ = 11.5 Hz, *C*H$_2$P), 34.0 (NCH$_2$*C*H$_2$), 20.2 (NCH$_2$CH$_2$*C*H$_2$), 13.9 (*C*H$_3$). $^{31}$P{$^1$H} NMR (121.49 MHz, CD$_2$Cl$_2$): $\delta$ −9.8.

 This journal is © The Royal Society of Chemistry 2016

Open Access Article. Published on 11 February 2016. Downloaded on 10/20/2025 7:02:02 PM.
This article is licensed under a Creative Commons Attribution 3.0 Unported Licence.

**Synthesis of [$Au_2Cl_2$(μ-P(*t*Bu)$_2$-NHC,κ*P*,κ*C*$^{NHC}$)] ([$Au_2Cl_2L^{tBu}$]).** To a solution of [$Ag_4Br_4(L^{tBu})_2$] (0.076 g, 0.052 mmol) in $CH_2Cl_2$ (5 mL) was added a solution of [AuCl(THT)] (4 equiv., 0.066 g, 0.21 mmol) in $CH_2Cl_2$ (2 mL) under protection against light. A white precipitate appeared instantaneously and the resulting suspension was stirred overnight. Filtration through Celite® and evaporation of the solvent afforded [$Au_2Cl_2L^{tBu}$] as a white powder. Yield: 0.083 g (0.10 mmol), 97%. Single crystals suitable for X-ray diffraction were obtained by slow vapour diffusion of $Et_2O$ in a $CH_2Cl_2$ solution of the complex. Anal. Calcd for $C_{22}H_{35}Au_2BrCl_2N_2P$ (823.34): C, 32.09; H, 4.28; N, 3.40. Found: C, 31.25; H, 4.13; N, 3.24. These experimental values fit better with the formula $C_{22}H_{35}Au_2Br_{0.5}Cl_{1.5}N_2P$ (845.57): C, 31.25; H, 4.17; N, 3.31, corresponding to partial halide exchange between AgBr and AuCl. $^1$H NMR (400.13 MHz, $CD_2Cl_2$): δ 7.89 (s, 1H, C*H*$_{arom.}$ H11), 7.74 (d, $^3J_{HH}$ = 1.6 Hz, 1H, C*H*$_{imid.}$), 7.73 (d, $^3J_{HH}$ = 7.9 Hz, 1H, C*H*$_{arom.}$ H7/H9), 7.55 (d, $^3J_{HH}$ = 7.9 Hz, 1H, C*H*$_{arom.}$ H9/H7), 7.47 (t, 1H, $^3J_{HH}$ = 7.9 Hz, 1H, C*H*$_{arom.}$ H8), 7.18 (d, $^3J_{HH}$ = 1.9 Hz, 1H, C*H*$_{imid.}$), 4.27 (t, $^3J_{HH}$ = 7.3 Hz, 2H, NC*H*$_2$), 3.37 (d, $^2J_{PH}$ = 11.0 Hz, 2H, C*H*$_2$P), 1.91 (quint, $^3J_{HH}$ = 7.4 Hz, 2H, NCH$_2$C*H*$_2$), 1.42 (sext, $^3J_{HH}$ = 7.4 Hz, 2H, NCH$_2$CH$_2$C*H*$_2$), 1.39 (d, $^3J_{PH}$ = 15.1 Hz, 18H, C(C*H*$_3$)$_3$), 0.99 (t, $^3J_{HH}$ = 7.4 Hz, 3H, C*H*$_3$). $^{13}$C{$^1$H} NMR (100.62 MHz, $CD_2Cl_2$): δ 170.3 (*C*$_{NHC}$), 140.0 (*C*$_{arom.}$), 138.6 (*C*$_{arom.}$), 131.3 (d, $J_{PC}$ = 5.8 Hz, *C*H$_{arom.}$), 130.1 (d, $J_{PC}$ = 1.6 Hz, *C*H$_{arom.}$), 127.5 (d, $J_{PC}$ = 7.0 Hz, *C*H$_{arom.}$), 124.4 (*C*H$_{arom.}$), 122.8 (*C*H$_{arom.}$), 121.4 (*C*H$_{arom.}$), 52.1 (N*C*H$_2$), 36.7 (d, $^1J_{PC}$ = 25.4 Hz, *C*(CH$_3$)$_3$), 33.3 (NCH$_2$*C*H$_2$), 29.9 (d, $^2J_{PC}$ = 4.8 Hz, C(*C*H$_3$)$_3$), 27.8 (d, $^1J_{PC}$ = 25.5 Hz, *C*H$_2$P), 20.1 (NCH$_2$CH$_2$*C*H$_2$), 13.8 (*C*H$_3$). $^{31}$P{$^1$H} NMR (161.98 MHz, $CD_2Cl_2$): δ 80.1 (minor) and 79.0 (major), due to the presence of chlorido and bromido derivatives, consistent with the elemental analysis data. HRMS (ESI$^+$): *m*/*z* calcd for $C_{22}H_{35}Au_2ClN_2P$ 787.1552, found 787.1547.

### X-ray crystallography

Suitable crystals for the X-ray analysis of all compounds were obtained as described above. Summary of the crystal data, data collection and refinement are given in Table S1 (see ESI‡).

Data sets for $L^{Ph}$·HBr, $L^{Cy}$·HBr·$BH_3$, [$Ag_4Br_4(L^{Ph})_2$], [$Ag_2(L^{Ph})_2](BF_4)_2$·$2CH_2Cl_2$, [$Cu_2Br_2(L^{Cy})_2$] and [$Au_2Cl_2L^{tBu}$] were collected at 173(2) K on a Bruker APEX-II CCD Duo diffractometer (graphite-monochromated Mo-Kα radiation, λ = 0.71073 Å). Data sets for [$Ag_2(L^{Ph})_2](BF_4)_2$, [$Ag_2(L^{tBu})_2](BF_4)_2$·$CH_2Cl_2$ and [$Cu_2Br_2(L^{tBu})_2$]·$2CH_2Cl_2$ were collected at 173(2) K on a Kappa CCD diffractometer (graphite-monochromated Mo-Kα radiation, λ = 0.71073 Å). Specific comments for each data set are given below. The cell parameters were determined using DENZO[43] (Kappa) or APEX2[44] (APEX-II) softwares. The structures were solved by direct methods using the program SHELXS-97 (compounds $L^{Cy}$·HBr·$BH_3$, $L^{Ph}$·HBr, [$Cu_2Br_2(L^{Cy})_2$] and [$Cu_2Br_2(L^{tBu})_2$]·$2CH_2Cl_2$) or SHELXS-2013 (complexes [$Ag_4Br_4(L^{Ph})_2$], [$Ag_2(L^{Ph})_2](BF_4)_2$·$2CH_2Cl_2$, [$Ag_2(L^{Ph})_2](BF_4)_2$, [$Ag_2(L^{tBu})_2](BF_4)_2$·$CH_2Cl_2$ and [$Au_2Cl_2L^{tBu}$]).[45] The refinement and all further calculations were carried out using SHELXL-97 (compound $L^{Ph}$·HBr, [$Cu_2Br_2(L^{Cy})_2$] and [$Cu_2Br_2(L^{tBu})_2$]·$2CH_2Cl_2$) or SHELXL-2013 (all other compounds).[45*b*] The H-atoms were introduced into the geometrically calculated positions (SHELXL-97 or SHELXL-2013 procedures) unless stated otherwise and refined riding on the corresponding parent atoms. The non-H atoms were refined anisotropically, using weighted full-matrix least-squares on $F^2$.

The following special comments apply to the models of the structures:

$L^{Cy}$·HBr·$BH_3$: the alkyl atoms C5, C6 and C7 are disordered on two positions.

$L^{Ph}$·HBr: A SQUEEZE procedure[46] was applied and the residual electron density was assigned to one half disordered molecule of $CH_2Cl_2$.

[$Ag_4Br_4(L^{Ph})_2$]: A SQUEEZE procedure[46] was applied and the residual electron density was assigned to one disordered molecule of ether.

[$Ag_2(L^{Ph})_2](BF_4)_2$: the alkyl atoms C31, C32 and C33 are disordered on two positions. A SQUEEZE procedure[46] was applied and the residual electron density was assigned to two disordered molecules of acetonitrile. The structure of this complex can be found in the ESI.‡

[$Ag_2(L^{tBu})_2](BF_4)_2$·$CH_2Cl_2$: thermal motions affect the alkyl chains on the ligands. The carbons atoms C49, C50 and C73 are disordered on two positions. The carbon atom C48 is also disordered on two positions but C48 and C48B have been imposed at the same position to avoid short-contacts between the H-atoms and subsequent alerts in the Checkcif. A SQUEEZE procedure[46] was applied and the residual electron density was assigned to one and a half disordered molecules of $CH_2Cl_2$.

[$Cu_2Br_2(L^{Cy})_2$]: The asymmetric unit contains one and a half molecules of the complex. The alkyl atoms C6 and C7 are disordered on two positions.

[$Cu_2Br_2(L^{tBu})_2$]·$2CH_2Cl_2$: The space group is chiral ($P2_1$) and the value of Flack parameter is −0.008(9). A SQUEEZE procedure[46] was applied and the residual electron density was assigned to one disordered molecule of toluene.

## Acknowledgements

The USIAS, CNRS, Unistra, Région Alsace and Communauté Urbaine de Strasbourg are acknowledged for the award of fellowships and a Gutenberg Excellence Chair (2010–11) to AAD. We thank the CNRS and the MESR (Paris) for funding and for a PhD grant to TS. We are grateful to Corinne Bailly and Dr Lydia Karmazin (Service de Radiocristallographie, Unistra) for solving crystal structures, and to Maurice Coppe and Dr Bruno Vincent (Service de Résonance Magnétique Nucléaire, Unistra) for assistance in the NMR studies. We thank Johnson Matthey PLC for a generous loan of gold precursors.

## References

1 (*a*) E. Peris and R. H. Crabtree, *Coord. Chem. Rev.*, 2004, **248**, 2239–2246; (*b*) L. Cavallo, A. Correa, C. Costabile and H. Jacobsen, *J. Organomet. Chem.*, 2005, **690**, 5407–5413;

Open Access Article. Published on 11 February 2016. Downloaded on 10/20/2025 7:02:02 PM.
This article is licensed under a Creative Commons Attribution 3.0 Unported Licence.

(*c*) R. H. Crabtree, *J. Organomet. Chem.*, 2005, **690**, 5451–5457.

2 (*a*) W. A. Herrmann and C. Köcher, *Angew. Chem., Int. Ed. Engl.*, 1997, **36**, 2162–2187; (*b*) J. C. Green, R. G. Scurr, P. L. Arnold and F. G. N. Cloke, *Chem. Commun.*, 1997, 1963–1964; (*c*) C. Boehme and G. Frenking, *Organometallics*, 1998, **17**, 5801–5809; (*d*) M.-T. Lee and C.-H. Hu, *Organometallics*, 2004, **23**, 976–983; (*e*) R. Tonner, G. Heydenrych and G. Frenking, *Chem. – Asian J.*, 2007, **2**, 1555–1567; (*f*) H. Jacobsen, A. Correa, A. Poater, C. Costabile and L. Cavallo, *Coord. Chem. Rev.*, 2009, **253**, 687–703; (*g*) A. Comas-Vives and J. N. Harvey, *Eur. J. Inorg. Chem.*, 2011, 5025–5035; (*h*) D. J. Nelson and S. P. Nolan, *Chem. Soc. Rev.*, 2013, **42**, 6723–6753.

3 (*a*) M. Scholl, S. Ding, C. W. Lee and R. H. Grubbs, *Org. Lett.*, 1999, **1**, 953–956; (*b*) W. A. Herrmann, V. P. W. Böhm, C. W. K. Gstöttmayr, M. Grosche, C.-P. Reisinger and T. Weskamp, *J. Organomet. Chem.*, 2001, **617–618**, 616–628; (*c*) G. D. Frey, J. Schütz, E. Herdtweck and W. A. Herrmann, *Organometallics*, 2005, **24**, 4416–4426; (*d*) A. Flahaut, S. Roland and P. Mangeney, *J. Organomet. Chem.*, 2007, **692**, 5754–5762; (*e*) V. Jurčík, S. P. Nolan and C. S. J. Cazin, *Chem. – Eur. J.*, 2009, **15**, 2509–2511; (*f*) T. E. Schmid, D. C. Jones, O. Songis, O. Diebolt, M. R. L. Furst, A. M. Z. Slawin and C. S. J. Cazin, *Dalton Trans.*, 2013, **42**, 7345–7353; (*g*) J. Broggi, V. Jurčík, O. Songis, A. Poater, L. Cavallo, A. M. Z. Slawin and C. S. J. Cazin, *J. Am. Chem. Soc.*, 2013, **135**, 4588–4591; (*h*) K. Farrell, H. Müller-Bunz and M. Albrecht, *Organometallics*, 2015, **34**, 5723–5733.

4 (*a*) F. Lazreg, A. M. Z. Slawin and C. S. J. Cazin, *Organometallics*, 2012, **31**, 7969–7975; (*b*) S. Guo, M. H. Lim and H. V. Huynh, *Organometallics*, 2013, **32**, 7225–7233.

5 (*a*) P. G. Edwards and F. E. Hahn, *Dalton Trans.*, 2011, **40**, 10278–10288; (*b*) S. Gaillard and J.-L. Renaud, *Dalton Trans.*, 2013, **42**, 7255–7270; (*c*) P. Hofmann and M. Brill, in *Molecular Catalysts*, Wiley-VCH Verlag GmbH & Co. KGaA, 2014, pp. 207–234.

6 (*a*) C. Yang, H. M. Lee and S. P. Nolan, *Org. Lett.*, 2001, **3**, 1511–1514; (*b*) N. Tsoureas, A. A. Danopoulos, A. A. D. Tulloch and M. E. Light, *Organometallics*, 2003, **22**, 4750–4758; (*c*) H. M. Lee, P. L. Chiu and J. Y. Zeng, *Inorg. Chim. Acta*, 2004, **357**, 4313–4321; (*d*) A.-E. Wang, J.-H. Xie, L.-X. Wang and Q.-L. Zhou, *Tetrahedron*, 2005, **61**, 259–266; (*e*) R. Hodgson and R. E. Douthwaite, *J. Organomet. Chem.*, 2005, **690**, 5822–5831; (*f*) F. E. Hahn, M. C. Jahnke and T. Pape, *Organometallics*, 2006, **25**, 5927–5936; (*g*) J. Zhong, J.-H. Xie, A.-E. Wang, W. Zhang and Q.-L. Zhou, *Synlett*, 2006, 1193–1196; (*h*) X. Quan, S. Kerdphon and P. G. Andersson, *Chem. – Eur. J.*, 2015, **21**, 3576–3579.

7 C. A. Wheaton, J.-P. J. Bow and M. Stradiotto, *Organometallics*, 2013, **32**, 6148–6161.

8 J. Witt, A. Pöthig, F. E. Kühn and W. Baratta, *Organometallics*, 2013, **32**, 4042–4045.

9 (*a*) A. P. Marchenko, H. N. Koidan, A. N. Hurieva, O. V. Gutov, A. N. Kostyuk, C. Tubaro, S. Lollo, A. Lanza, F. Nestola and A. Biffis, *Organometallics*, 2013, **32**, 718–721; (*b*) P. Nägele, U. Herrlich, F. Rominger and P. Hofmann, *Organometallics*, 2013, **32**, 181–191; (*c*) P. Ai, A. A. Danopoulos, P. Braunstein and K. Yu Monakhov, *Chem. Commun.*, 2014, **50**, 103–105; (*d*) C. C. Brown, F. Rominger, M. Limbach and P. Hofmann, *Inorg. Chem.*, 2015, **54**, 10126–10140; (*e*) P. Ai, A. A. Danopoulos and P. Braunstein, *Inorg. Chem.*, 2015, **54**, 3722–3724.

10 (*a*) W. A. Herrmann, C. Köcher, L. J. Gooßen and G. R. J. Artus, *Chem. – Eur. J.*, 1996, **2**, 1627–1636; (*b*) A. A. Danopoulos, S. Winston, T. Gelbrich, M. B. Hursthouse and R. P. Tooze, *Chem. Commun.*, 2002, 482–483; (*c*) J. Wolf, A. Labande, J.-C. Daran and R. Poli, *J. Organomet. Chem.*, 2006, **691**, 433–443; (*d*) J. Wolf, A. Labande, J.-C. Daran and R. Poli, *Eur. J. Inorg. Chem.*, 2008, 3024–3030; (*e*) G. Song, X. Li, Z. Song, J. Zhao and H. Zhang, *Chem. – Eur. J.*, 2009, **15**, 5535–5544; (*f*) E. Kühnel, I. V. Shishkov, F. Rominger, T. Oeser and P. Hofmann, *Organometallics*, 2012, **31**, 8000–8011; (*g*) M. Brill, E. Kühnel, C. Scriban, F. Rominger and P. Hofmann, *Dalton Trans.*, 2013, **42**, 12861–12864; (*h*) M. Brill, D. Marrwitz, F. Rominger and P. Hofmann, *J. Organomet. Chem.*, 2015, **775**, 137–151.

11 (*a*) E. Bappert and G. Helmchen, *Synlett*, 2004, 1789–1793; (*b*) C.-C. Ho, S. Chatterjee, T.-L. Wu, K.-T. Chan, Y.-W. Chang, T.-H. Hsiao and H. M. Lee, *Organometallics*, 2009, **28**, 2837–2847; (*c*) I. Abdellah, Y. Canac, C. D. Mboyi, C. Duhayon and R. Chauvin, *J. Organomet. Chem.*, 2015, **776**, 149–152.

12 (*a*) M. Raynal, X. Liu, R. Pattacini, C. Vallée, H. Olivier-Bourbigou and P. Braunstein, *Dalton Trans.*, 2009, 7288–7293; (*b*) B. Vabre, Y. Canac, C. Duhayon, R. Chauvin and D. Zargarian, *Chem. Commun.*, 2012, **48**, 10446–10448; (*c*) X. Liu and P. Braunstein, *Inorg. Chem.*, 2013, **52**, 7367–7379; (*d*) B. Vabre, Y. Canac, C. Lepetit, C. Duhayon, R. Chauvin and D. Zargarian, *Chem. – Eur. J.*, 2015, **21**, 17403–17414; (*e*) T. Simler, P. Braunstein and A. A. Danopoulos, *Angew. Chem., Int. Ed.*, 2015, **54**, 13691–13695.

13 (*a*) H. M. Lee, J. Y. Zeng, C.-H. Hu and M.-T. Lee, *Inorg. Chem.*, 2004, **43**, 6822–6829; (*b*) S. Gischig and A. Togni, *Organometallics*, 2005, **24**, 203–205; (*c*) T. Steinke, B. K. Shaw, H. Jong, B. O. Patrick and M. D. Fryzuk, *Organometallics*, 2009, **28**, 2830–2836; (*d*) D. A. Valyaev, O. A. Filippov, N. Lugan, G. Lavigne and N. A. Ustynyuk, *Angew. Chem., Int. Ed.*, 2015, **54**, 6315–6319.

14 The Cambridge Structural Database, accessed Jan. 2016: F. Allen, *Acta Crystallogr., Sect. B: Struct. Sci.*, 2002, **58**, 380–388.

15 (*a*) P. L. Chiu and H. M. Lee, *Organometallics*, 2005, **24**, 1692–1702; (*b*) H. Salem, M. Schmitt, U. Herrlich, E. Kühnel, M. Brill, P. Nägele, A. L. Bogado, F. Rominger and P. Hofmann, *Organometallics*, 2013, **32**, 29–46; (*c*) A. Marchenko, H. Koidan, A. Hurieva, O. Kurpiieva, Y. Vlasenko, A. Kostyuk, C. Tubaro, A. Lenarda, A. Biffis and C. Graiff, *J. Organomet. Chem.*, 2014, **771**, 14–23.

16 H. M. J. Wang and I. J. B. Lin, *Organometallics*, 1998, **17**, 972–975.

 This journal is © The Royal Society of Chemistry 2016

Open Access Article. Published on 11 February 2016. Downloaded on 10/20/2025 7:02:02 PM.
This article is licensed under a Creative Commons Attribution 3.0 Unported Licence.

17 M. E. Humphries, W. H. Pecak, S. A. Hohenboken, S. R. Alvarado, D. C. Swenson and G. J. Domski, *Inorg. Chem. Commun.*, 2013, **37**, 138–143.
18 J. Y. Zeng, M.-H. Hsieh and H. M. Lee, *J. Organomet. Chem.*, 2005, **690**, 5662–5671.
19 S. Bestgen, M. T. Gamer, S. Lebedkin, M. M. Kappes and P. W. Roesky, *Chem. – Eur. J.*, 2015, **21**, 601–614.
20 D. Hérault, D. H. Nguyen, D. Nuel and G. Buono, *Chem. Soc. Rev.*, 2015, **44**, 2508–2528.
21 (*a*) A. A. Danopoulos, N. Tsoureas, S. A. Macgregor and C. Smith, *Organometallics*, 2007, **26**, 253–263; (*b*) G. Song, X. Wang, Y. Li and X. Li, *Organometallics*, 2008, **27**, 1187–1192.
22 (*a*) T. Steiner, *Acta Crystallogr., Sect. B: Struct. Sci.*, 1998, **54**, 456–463; (*b*) T. Steiner and G. R. Desiraju, *Chem. Commun.*, 1998, 891–892; (*c*) T. Steiner, *Angew. Chem., Int. Ed.*, 2002, **41**, 48–76; (*d*) A. Kovács and Z. Varga, *Coord. Chem. Rev.*, 2006, **250**, 710–727.
23 V. Charra, P. de Frémont, P.-A. R. Breuil, H. Olivier-Bourbigou and P. Braunstein, *J. Organomet. Chem.*, 2015, **795**, 25–33.
24 D. Tapu, D. A. Dixon and C. Roe, *Chem. Rev.*, 2009, **109**, 3385–3407.
25 (*a*) J. C. Garrison and W. J. Youngs, *Chem. Rev.*, 2005, **105**, 3978–4008; (*b*) J. C. Y. Lin, R. T. W. Huang, C. S. Lee, A. Bhattacharyya, W. S. Hwang and I. J. B. Lin, *Chem. Rev.*, 2009, **109**, 3561–3598.
26 W. D. Clark, G. E. Tyson, T. K. Hollis, H. U. Valle, E. J. Valente, A. G. Oliver and M. P. Dukes, *Dalton Trans.*, 2013, **42**, 7338–7344.
27 X. Hu, I. Castro-Rodriguez, K. Olsen and K. Meyer, *Organometallics*, 2004, **23**, 755–764.
28 H.-L. Su, L. M. Pérez, S.-J. Lee, J. H. Reibenspies, H. S. Bazzi and D. E. Bergbreiter, *Organometallics*, 2012, **31**, 4063–4071.
29 A. Bondi, *J. Phys. Chem.*, 1964, **68**, 441–451.
30 (*a*) S. Sculfort and P. Braunstein, *Chem. Soc. Rev.*, 2011, **40**, 2741–2760; (*b*) H. Schmidbaur and A. Schier, *Angew. Chem., Int. Ed.*, 2015, **54**, 746–784.
31 (*a*) B.-K. Teo and J. C. Calabrese, *J. Chem. Soc., Chem. Commun.*, 1976, 185–186; (*b*) G. J. S. Venter, A. Roodt and R. Meijboom, *Inorg. Chim. Acta*, 2009, **362**, 2475–2479.
32 T. A. P. Paulose, S.-C. Wu, J. A. Olson, T. Chau, N. Theaker, M. Hassler, J. W. Quail and S. R. Foley, *Dalton Trans.*, 2012, **41**, 251–260.
33 B.-K. Teo and J. C. Calabrese, *Inorg. Chem.*, 1976, **15**, 2467–2474.
34 (*a*) D. J. Nielsen, K. J. Cavell, B. W. Skelton and A. H. White, *Inorg. Chim. Acta*, 2002, **327**, 116–125; (*b*) D. Qin, X. Zeng, Q. Li, F. Xu, H. Song and Z.-Z. Zhang, *Chem. Commun.*, 2007, 147–149; (*c*) F. Jean-Baptiste dit Dominique, H. Gornitzka and C. Hemmert, *J. Organomet. Chem.*, 2008, **693**, 579–583; (*d*) C. E. Willans, K. M. Anderson, M. J. Paterson, P. C. Junk, L. J. Barbour and J. W. Steed, *Eur. J. Inorg. Chem.*, 2009, 2835–2843; (*e*) A. Rit, T. Pape and F. E. Hahn, *Organometallics*, 2011, **30**, 6393–6401.
35 (*a*) J. M. Jenkins and B. L. Shaw, *J. Chem. Soc. A*, 1966, 770–775; (*b*) A. Pidcock, *Chem. Commun.*, 1968, 92–92.
36 (*a*) A. J. Arduengo III, H. V. R. Dias, J. C. Calabrese and F. Davidson, *Organometallics*, 1993, **12**, 3405–3409; (*b*) B. Bildstein, M. Malaun, H. Kopacka, K. Wurst, M. Mitterböck, K.-H. Ongania, G. Opromolla and P. Zanello, *Organometallics*, 1999, **18**, 4325–4336; (*c*) S. Hameury, P. de Frémont, P.-A. R. Breuil, H. Olivier-Bourbigou and P. Braunstein, *Dalton Trans.*, 2014, **43**, 4700–4710.
37 (*a*) R. G. Pearson, *Inorg. Chem.*, 1973, **12**, 712–713; (*b*) S. Fuertes, A. J. Chueca and V. Sicilia, *Inorg. Chem.*, 2015, **54**, 9885–9895.
38 A. A. Danopoulos, P. Cole, S. P. Downing and D. Pugh, *J. Organomet. Chem.*, 2008, **693**, 3369–3374.
39 (*a*) A. A. D. Tulloch, A. A. Danopoulos, S. Kleinhenz, M. E. Light, M. B. Hursthouse and G. Eastham, *Organometallics*, 2001, **20**, 2027–2031; (*b*) N. Schneider, V. César, S. Bellemin-Laponnaz and L. H. Gade, *J. Organomet. Chem.*, 2005, **690**, 5556–5561; (*c*) J. Broggi, S. Díez-González, J. L. Petersen, S. Berteina-Raboin, S. P. Nolan and L. A. Agrofoglio, *Synthesis*, 2008, 141–148; (*d*) I. V. Shishkov, F. Rominger and P. Hofmann, *Dalton Trans.*, 2009, 1428–1435; (*e*) S. Simonovic, A. C. Whitwood, W. Clegg, R. W. Harrington, M. B. Hursthouse, L. Male and R. E. Douthwaite, *Eur. J. Inorg. Chem.*, 2009, 1786–1795; (*f*) M. Bessel, F. Rominger and B. F. Straub, *Synthesis*, 2010, 1459–1466; (*g*) S. Díez-González, E. C. Escudero-Adán, J. Benet-Buchholz, E. D. Stevens, A. M. Z. Slawin and S. P. Nolan, *Dalton Trans.*, 2010, **39**, 7595–7606; (*h*) M. Slivarichova, R. Ahmad, Y.-Y. Kuo, J. Nunn, M. F. Haddow, H. Othman and G. R. Owen, *Organometallics*, 2011, **30**, 4779–4787; (*i*) C. E. Strasser and V. J. Catalano, *Inorg. Chem.*, 2011, **50**, 11228–11234; (*j*) B. R. M. Lake, E. K. Bullough, T. J. Williams, A. C. Whitwood, M. A. Little and C. E. Willans, *Chem. Commun.*, 2012, **48**, 4887–4889; (*k*) B. Liu, C. Chen, Y. Zhang, X. Liu and W. Chen, *Organometallics*, 2013, **32**, 5451–5460; (*l*) B. R. M. Lake and C. E. Willans, *Chem. – Eur. J.*, 2013, **19**, 16780–16790.
40 P. de Frémont, N. M. Scott, E. D. Stevens and S. P. Nolan, *Organometallics*, 2005, **24**, 2411–2418.
41 (*a*) S. Gambarotta, C. Floriani, A. Chiesi-Villa and C. Guastini, *J. Chem. Soc., Chem. Commun.*, 1983, 1156–1158; (*b*) M. Stollenz and F. Meyer, *Organometallics*, 2012, **31**, 7708–7727.
42 R. Uson, A. Laguna, M. Laguna, D. A. Briggs, H. H. Murray and J. P. Fackler, in *Inorganic Syntheses*, John Wiley & Sons, Inc., 2007, vol. 26, pp. 85–91.
43 R. W. W. Hooft, *DENZO and COLLECT*, Nonius BV, Delft, The Netherlands, 1998.
44 *APEX2, SAINT and SADABS*, Bruker AXS Inc., Madison, Wisconsin, USA, 2009.
45 (*a*) G. M. Sheldrick, *Acta Crystallogr., Sect. A: Fundam. Crystallogr.*, 2008, **64**, 112–122; (*b*) G. M. Sheldrick, *SHELX2013*, University of Göttingen, Germany, 2013.
46 A. Spek, *J. Appl. Crystallogr.*, 2003, **36**, 7–13.